Department of Radio Science and Engineering

Reliable and Efficient Numerical Methods for Time Harmonic Electromagnetic Design Problems

Juhani Kataja

Aalto University

DOCTORAL DISSERTATIONS

Aalto University publication series
DOCTORAL DISSERTATIONS 155/2014

Reliable and Efficient Numerical Methods for Time Harmonic Electromagnetic Design Problems

Juhani Kataja

A doctoral dissertation completed for the degree of Doctor of Science (Technology) (Doctor of Philosophy) to be defended, with the permission of the Aalto University School of Electrical Engineering, at a public examination held at the lecture hall S1 of the school on 24 October 2014 at 12.

Aalto University
School of Electrical Engineering
Department of Radio Science and Engineering
Computational electromagnetics

Supervising professor
Keijo Nikoskinen

Thesis advisor
Pasi Ylä-Oijala

Preliminary examiners
Mats Gustafsson, Lund University, Sweden
Jussi Rahola, Optenni Oy, Finland

Aalto University publication series
DOCTORAL DISSERTATIONS 155/2014

ISBN 978-952-60-5898-6
ISBN 978-952-60-5899-3 (pdf)
ISSN-L 1799-4934
ISSN 1799-4934 (printed)
ISSN 1799-4942 (pdf)
http://urn.fi/URN:ISBN:978-952-60-5899-3

Unigrafia Oy
Helsinki 2014

Finland

441 697
Printed matter

Aalto University

Abstract

Aalto University, P.O. Box 11000, FI-00076 Aalto www.aalto.fi

Author
Juhani Kataja

Name of the doctoral dissertation
Reliable and efficient numerical methods for time harmonic electromagnetic design problems

Publisher School of Electrical Engineering

Unit Department of Radio Science and Engineering

Series Aalto University publication series DOCTORAL DISSERTATIONS 155/2014

Field of research Electromagnetics

Manuscript submitted 12 December 2013 **Date of the defence** 24 October 2014

Permission to publish granted (date) 28 February 2014 **Language** English

☐ **Monograph** ☒ **Article dissertation (summary + original articles)**

Abstract

This dissertation studies numerical methods for solving time-harmonic Maxwell's equations. In this work, boundary element and a least squares type finite element method for time-harmonic Maxwell's equations is analysed.

The boundary element method is studied from the point of view of shape optimization and shape sensitivity analysis. The main result of the dissertation is the description how to calculate numerically the derivative of electromagnetic properties of a metallic scatterer with respect to variation of its shape. The motivation of the result is the adjoint variable method aimed at computing the derivative of a cost function of a generic optimization problem. The method has the property that, essentially, it suffices to differentiate the system matrix with respect to shape if the load functional or the cost functional do not depend on the shape explicitly. The boundary element method is also applied in as wide as possible characterisation of the shapes of wire dipoles and that way in shape optimisation.

The least-squares finite-element method for time-harmonic Maxwell's equations results in a method where the system matrix is positive definite despite the underlying physics those of time-harmonic fields usually lead to strictly indefinite systems. The positive definiteness of the system matrix is inherited from the ellipticity of the sesquilinear form of the variational method. The implementation of a conformal discretization is not, however, always reasonable for the reason that in certain geometries the finite element solution vanishes on the boundary when only tangential, or normal, component is required to vanish. Therefore, the discrete solution space is widened in such a manner that on mesh dense enough the sesquilinear form is still elliptic and that the tangential, or normal, component vanishes in suitable weak sense.

Keywords Optimization, EFIE, boundary element method, finite element method

ISBN (printed) 978-952-60-5898-6 **ISBN (pdf)** 978-952-60-5899-3

ISSN-L 1799-4934 **ISSN (printed)** 1799-4934 **ISSN (pdf)** 1799-4942

Location of publisher Helsinki **Location of printing** Helsinki **Year** 2014

Pages 117 **urn** http://urn.fi/URN:ISBN:978-952-60-5899-3

Aalto-yliopisto

Tiivistelmä

Aalto-yliopisto, PL 11000, 00076 Aalto www.aalto.fi

Tekijä
Juhani Kataja

Väitöskirjan nimi
Luotettavia ja tehokkaita numeerisia menetelmiä aikaharmonisiin sähkömagneettisiin suunnittelutehtäviin

Julkaisija Sähkötekniikan korkeakoulu

Yksikkö Radiotieteen ja -tekniikan laitos

Sarja Aalto University publication series DOCTORAL DISSERTATIONS 155/2014

Tutkimusala Sähkömagnetiikka

Käsikirjoituksen pvm 12.12.2013 **Väitöspäivä** 24.10.2014

Julkaisuluvan myöntämispäivä 28.02.2014 **Kieli** Englanti

☐ **Monografia** ☒ **Yhdistelmäväitöskirja (yhteenveto-osa + erillisartikkelit)**

Tiivistelmä

Tämä työ käsittelee numeerisia menetelmiä aikaharmonisten sähkömagneettisten kenttien simuloinnissa. Työssä kehitetään reunaelementtimenetelmää sekä analysoidaan miten voidaan ratkaista Maxwellin aikaharmoniset yhtälöt duaalinormaaliyhtälöinä pienimmän neliösumman mielessä elementtimenetelmällä.

Reunaelementtimenetelmää työssä tarkastellaan muodon optimoinnin ja herkkyysanalyysin näkökulmasta. Työn päätulos kertoo miten lasketaan numeerisesti metallisten sirottajien sähköisten ominaisuuksien derivaatta sirottajan geometrian muutoksen suhteen. Tuloksen kannustimena on yleisen optimointitehtävän kustannusfunktion derivaatan laskentaan kehitetty abstrakti dualimuuttujamenetelmä. Menetellä on ominaisuus, joka takaa, että olennaisesti riittää laskea systeemimatriisin alkioiden muotoderivaatta kun ollaan kiinnostuneita optimointitehtävän kustannusfunktion derivaatasta, kun lastifunktionaali ja kustannusfunktio eivät riipu eksplisiittisesti sirottajan muodosta. Reunaelementtimenetelmää sovelletaan työssä myös lankadipolien muodon mahdollisimman laajan parametriavaruuden karakterisointiin, ja sitä kautta muodon optimointiin.

Pienimmän neliösumman elementtimenetelmä aikaharmonisille Maxwellin yhtälöille johtaa menetelmään, jossa systeemimatriisi on positiividefiniitti vaikka tavallisesti aikaharmoniset yhtälöt johtavat aidosti indefiniitteihin järjestelmiin. Systeemimatriisin positiividefiniittiys periytyy variaatiotehtävän seskvilineaarimuodon elliptisyydestä. Konformin diskretoinnin toteuttaminen ei kuitenkaan ole aina järkevää, sillä tietynlaisissa alueissa se johtaa elementtiratkaisuihin, jotka häviävät reunalla kokonaan kun vain tangentiaalisen tai normaalin osan tulisi hävitä. Työssä lavennetaan ratkaisuavaruuttaa sopivasti siten, että tarpeeksi tiheällä verkolla seskvilineaarimuoto on edelleen elliptinen ja elementtiratkaisu toteuttaa reunaehdon heikommassa mielessä.

Avainsanat Optimointi, reunaelementtimenetelmä, EFIE, elementtimenetelmä

ISBN (painettu) 978-952-60-5898-6 **ISBN (pdf)** 978-952-60-5899-3

ISSN-L 1799-4934 **ISSN (painettu)** 1799-4934 **ISSN (pdf)** 1799-4942

Julkaisupaikka Helsinki **Painopaikka** Helsinki **Vuosi** 2014

Sivumäärä 117 **urn** http://urn.fi/URN:ISBN:978-952-60-5899-3

Contents

List of Publications

This thesis consists of an overview and of the following publications which are referred to in the text by their Roman numerals.

I J. Kataja, and K. Nikoskinen. The parametric optimization of wire dipole antennas. *IEEE Transactions on Antennas and Propagation*, vol. 59, no. 2, pp. 350–356, Feb. 2011.

II J. Kataja, A.G. Polimeridis, J.R. Mosig and P. Ylä-Oijala. Analytical shape derivatives of the MFIE system matrix discretized with RWG functions. *IEEE Transactions on Antennas and Propagation*, vol. 61, no. 2, pp. 985–988, Feb. 2013.

III J. Kataja and J.I. Toivanen. On shape differentiation of discretized electric field integral equation. *Engineering Analysis with Boundary Elements*, vol. 37, no. 9, pp. 1197–1203, Sept. 2013.

IV J. Kataja, S. Järvenpää, Jukka I. Toivanen, Raino A.E. Mäkinen, Pasi Ylä-Oijala. Shape sensitivity analysis and gradient based optimization of large structures using MLFMA. *IEEE Transactions on Antennas and Propagation*, accepted, 2014.

V J. Kataja. A least squares finite element method for the extended Maxwell system. *Progress in Electromagnetic Research M*, vol. 33, pp. 137–151, 2013.

Author's Contribution

Publication I: "The parametric optimization of wire dipole antennas"

This publication is an extension of a chapter of the author's M.Sc. thesis where directivities of Landstorfer's wire antennas were re-optimized. The idea to study the Landstorfer type antennas was suggested by Prof. Keijo Nikoskinen, otherwise the author is the main contributor of the Publication I.

Publication II: "Analytical shape derivatives of the MFIE system matrix discretized with RWG functions"

The author derived the derivative formulas described in this paper. The rest of the paper was made in close a collaboration with the second author Dr. Athanasios Polimeridis. The singularity cancellation quadratures were implemented by Dr. Polimeridis. The rest of the implementation and analysis were carried out by the author.

Publication III: "On shape differentiation of discretized electric field integral equation"

This paper was a result of a close collaboration with Dr. Toivanen who provided an implementation for the automatic differentiation routines of the electric field integral equation. The author derived the shape derivative formulas and wrote most of the manuscript. Dr. Seppo Järvenpää provided assistance with an efficient C++ implementation of the method for the PIFA antenna example.

Publication IV: "Shape sensitivity analysis and gradient based optimization of large structures using MLFMA"

This article resulted from a close collaboration with Dr. Seppo Järvenpää. The author derived the shape derivative formulas and implemented them on the non-differentiated MLFMA code written by Järvenpää. The authors Toivanen, Mäkinen and Ylä-Oijala provided substantial insight into the paper. Furthermore, this is continuation of the Publication III.

Publication V: "A least squares finite element method for the extended Maxwell system"

The author is the sole contributor of the publication. The idea to study the extended Maxwell system was suggested by Dr. Matti Taskinen.

Preface

This dissertation is the result of the work that was carried out at the Department of Radio Science and Engineering at the Aalto University School of Electrical Engineering.

I am grateful to my supervisor Prof. Keijo Nikoskinen for supporting me in the pursuit of this doctoral dissertation and kindly providing his insight to which direction the work could be taken in few occasions. I wish to thank my advisor Dr. Pasi Ylä-Oijala for commenting the present work during last years and for sharing his invaluable expertise on surface integral equations and computational electromagnetics at large.

I wish to thank the pre-examiners Prof. Mats Gustafsson and Dr. Jussi Rahola for their efforts and for excellent comments about the work. I am honoured to have Prof. Erkki Somersalo to act as the opponent in the public examination of this dissertation.

I thank Dr. Seppo Järvenpää especially for sharing his highly practical expertise on fast multipole methods and for numerous interesting discussions about programming and other subjects as well. The collaboration with Dr. Jukka Toivanen, Dr. Athanasios Polimeridis, Prof. Raino Mäkinen and Prof. Juan Mosig has been very fruitful. Their insights have had a great positive impact on the quality of this dissertation. For that, I am truly grateful. I thank Dr. Matti Taskinen for sharing his expertise on the extended Maxwell's system. Also, I wish thank the anonymous reviewers who volunteered to comment the publications of this dissertation and who thus helped to raise their quality.

I also wish to thank the coworkers at the Department of Radio Science and Engineering for creating an enjoyable working atmosphere and for in-depth discussions regarding, albeit not restricted to, electromagnetics and numerics. It has been a privilege to be surrounded by people who are experts in their fields.

I thank my friends for being so awesome.

Finally, I wish to express my deepest and warmest gratitude to my family. Without your support this book would not exist.

Espoo, October 6, 2014,

Juhani Kataja

List of abbreviations and symbols

Abbreviations

BEM	Boundary element method
BFGS	Broyden-Fletcher-Goldfarb-Shanno
CEM	Computational electromagnetics
EFIE	Electric field integral equation
FD	Finite difference
FE	Finite element
FEM	Finite element method
FFT	Fast fourier transform
FOSLL^*	First order system LL^*
MFIE	Magnetic field integral equation
MLFMA	Multi-level fast multipole algorithm
MoM	Method of moments
PEC	Perfect electric conductor
PIFA	Planar inverted F antenna
PMC	Perfect magnetic conductor
RT	Raviart-Thomas
RWG	Rao-Wilton-Glisson
SVD	Singular value decomposition

Symbols

$f * g$	Convolution of f and g
a.e.	Almost everywhere
∇	Gradient
$\nabla\times$	Curl
$\nabla\cdot$	Divergence
$\nabla_\Gamma\cdot$	Surface divergence on Γ
$\partial\Omega$	Boundary of set

(u, v)	Interior product of u and v
$U^\perp$	Orthogonal complement of U
V'	Space of continuous linear functionals on V
$S_1 \times S_2$	Cartesian product of two sets
δ	Dirac's delta function
δ_Γ	Dirac's delta distribution supported by Γ
dist	Distance function
η	Wave impedance in homogeneous isotropic medium
spt	Support of function
χ_Ω	Indicator function of Ω
A	Ampere
$C_0^\infty(D)$	Set of smooth compactly supported functions on D
$\mathcal{D}(L)$	Domain of L
$d\sigma_x$	Surface measure in variable x
$\mathcal{E}'$	Space of compactly supported distributions
$\mathbf{A}^H$	Hermitian transpose of matrix $\mathbf{A}$
m	Meter
$\mathcal{N}(T)$	Kernel of T
$\mathcal{RT}(\Gamma)$	Raviart-Thomas function space on Γ
s	Second
$S_{h,k}$	Nodal Lagrange finite element space of polynomial order k on mesh with triangles having size h
V	Volt

1. Introduction

Maxwell's equations [1, 2] provide us with a really good theory explaining and modelling electromagnetic interactions, which clearly are the most prevalent physical phenomena in our daily lives. The theory predicts elegantly how electric charges and currents interact in the presence of medium.

However elegant the equations may be, they lead to very complicated mathematical models, even after rather striking idealisations, such as linearisation, homogenisation of the material or restriction of the computational domain of interest with boundary conditions. The medium and the shape of the domain is what makes the equations so complicated and just that–the need to model general media and domains–calls for computer aided numerical methods.

Whether or not a specific method is effective to a given problem is determined by *efficiency* and *reliability* of the method. That is to ask: Does the method provide a solution accurate enough within a time frame short enough? Lately, the number of algorithms, not forgetting the concrete solution codes, for which the answer is yes has increased dramatically. In fact, the advance in numerical solution methods together with development of computers has had a major impact in engineering and design.

In the field of computational electromagnetics there are three fundamentally different approaches to solve Maxwell's equations, each excelling in their own domain of feasible problems: finite element method, finite-difference time-domain method and boundary element method. Although the finite element method is a general procedure to discretize variational problems, in computational electromagnetics it usually refers to a class of methods where a variational problem directly derived from Maxwell's equations is discretized. In contrast, in the boundary element methods the problem is first reduced to an integro-differential equation on the boundary

of the domain before discretization by finite element method or some other scheme. The finite-difference time-domain method, on the other hand, replaces all the derivatives appearing in Maxwell's equations with difference approximations. This thesis contributes to boundary element methods and finite element methods in computational electromagnetics.

In boundary element methods, shape optimization techniques are developed further: A physically reasonable shape parametrization for wire dipole antennas is developed and applied to optimization of directivity and input impedance. Also the computation of the shape derivatives appearing in the discretized electric and magnetic field integral equation is addressed. In particular, the change of variables method [3] is applied in calculating a closed-form expression for the derivatives of the system matrices. The motive for computing the shape derivative comes from the steepest descent method of non-constrained optimization: at each iteration, the derivative gives further information in which direction the next iterate should be. Furthermore, when a designer has arrived to some particular design, the shape derivative can be used to efficiently calculate its sensitivity to infinitesimal perturbations of the geometry.

The finite element method is contributed by extending least squares finite element method and especially first order system LL^* method [4, 5] to time-harmonic Maxwell's equations. Furthermore, a link is drawn between the first order system LL^* method and the extended Maxwell's equations proposed by Picard in 1985 [6]. The developed finite element methods exhibits good stability properties at static frequency limit.

The thesis is organized as follows. After the introduction, Maxwell's equations, the extended equations proposed by Picard and boundary conditions are presented in order to fix notation. In Chapter 3 boundary element methods for electromagnetic scattering problems are reviewed. After that, in Chapter 4, motivational background of shape optimization in electromagnetics for the Publications I–IV is discussed. Following that, in Chapter 5 the LL^* least squares finite element method is reviewed briefly together with the extended Maxwell's equations. Finally, a short summary of each of the publications is presented.

2. Maxwell's equations

The macroscopic Maxwell's equations describe the connection between scalar charge and vectorial current densities ρ and $\mathbf{J}$, and electric and magnetic fields and flux densities $\mathbf{E}$, $\mathbf{H}$, $\mathbf{D}$ and $\mathbf{B}$, each being a vector field on $\mathbb{R}^3$ [7]. The equations are

$$\nabla \times \mathbf{H} - \frac{\partial}{\partial t}\mathbf{D} = \mathbf{J} \tag{2.1}$$

$$\nabla \cdot \mathbf{D} = \rho \tag{2.2}$$

$$\nabla \times \mathbf{E} + \frac{\partial}{\partial t}\mathbf{B} = 0 \tag{2.3}$$

$$\nabla \cdot \mathbf{B} = 0 \tag{2.4}$$

The charge and current must satisfy the conservation equation

$$\nabla \cdot \mathbf{J} + \frac{\partial}{\partial t}\rho = 0, \tag{2.5}$$

from which actually (2.1) and (2.2) follow by interpreting the charge and current densities as differential 3-forms in 4-dimensional space-time [8].

The force exerted to a particle having charge q and velocity $\mathbf{v}$ is determined by the Lorentz force equation

$$\mathbf{F} = q(\mathbf{E} + \mathbf{v} \times \mathbf{B}) \tag{2.6}$$

On a microscropic level, the electric and magnetic fields $\mathbf{E}$ and $\mathbf{B}$ are related to the flux densities $\mathbf{D}$ and $\mathbf{H}$ by the *permittivity* and *permeability* of vacuum, denoted by ε_0 and μ_0, respectively. The relation is linear in the classical electrodynamic theory [7]:

$$\begin{cases} \mathbf{D} = \varepsilon_0 \mathbf{E} \\ \mathbf{B} = \mu_0 \mathbf{H}, \end{cases} \tag{2.7}$$

The values for the permittivity and permeability of vacuum are

$$\varepsilon_0 = 8.854\,187\,8\cdots \times 10^{-12}\ \frac{\mathrm{As}}{\mathrm{Vm}} \quad \text{and} \tag{2.8}$$

$$\mu_0 = 4\pi \cdot 10^{-7}\ \frac{\mathrm{Vs}}{\mathrm{Am}}. \tag{2.9}$$

On the other hand, the relation between averaged macroscopic fields can be very complicated, e.g. non-linear, non-isotropic or even hysteritic, such as in many ferromagnetic materials. Thus, the dependency is often written in a general form:

$$\begin{cases} \mathbf{D} = \mathbf{D}(\mathbf{E}, \mathbf{H}) \\ \mathbf{B} = \mathbf{B}(\mathbf{E}, \mathbf{H}). \end{cases} \tag{2.10}$$

In isotropic linear non-dispersive medium the fields and flux densities relate as

$$\begin{cases} \mathbf{D} = \varepsilon \mathbf{E} \quad \text{and} \\ \mathbf{B} = \mu \mathbf{H}, \end{cases} \tag{2.11}$$

where ε and μ are scalar quantities. In this dissertation, material relation given by (2.11) is assumed.

Taking Fourier transform in time from (2.1)–(2.4), (or assuming sinusoidal time behaviour) Maxwell's equations for the time-harmonic fields are

$$\nabla \times \mathbf{H} + i\omega\varepsilon \mathbf{E} = \mathbf{J} \tag{2.12}$$

$$\nabla \cdot \varepsilon \mathbf{E} = \rho \tag{2.13}$$

$$\nabla \times \mathbf{E} - i\omega\mu \mathbf{H} = 0 \tag{2.14}$$

$$\nabla \cdot \mu \mathbf{H} = 0, \tag{2.15}$$

where i is the imaginary unit and ω is the angular frequency given, in terms of frequency f, by $\omega = 2\pi f$.

When the frequency is not zero, the equations (2.13) and (2.15) follow from (2.12) and (2.14). Thus, it suffices to consider the reduced time-harmonic system

$$\left(\begin{bmatrix} 0 & \nabla\times \\ -\nabla\times & 0 \end{bmatrix} + \begin{bmatrix} i\omega\varepsilon & 0 \\ 0 & i\omega\mu \end{bmatrix} \right) \begin{bmatrix} \mathbf{E} \\ \mathbf{H} \end{bmatrix} = \begin{bmatrix} \mathbf{J} \\ \mathbf{M} \end{bmatrix}, \tag{2.16}$$

where M is a fictitious magnetic current. This system is the basis for boundary integral equations discussed in Section 3.3.

However, the principal part, i.e. the part having highest order derivatives, of the operator equation appearing in (2.16) has an infinite dimensional nullspace consisting of conservative fields. Thus one would expect that at the limit $\omega \to 0$ all numerical algorithms based on (2.16) become unstable. Such a *low-frequency breakdown* phenomenon is indeed a concern in both boundary integral equations [9, 10] and in finite element methods [11].

The low-frequency breakdown can be circumvented in the operator level by inspecting the extended Maxwell's equations [6, 12, 13]. To that end, the field variables are normalized:

$$\hat{\mathbf{E}} = \sqrt{\varepsilon}\mathbf{E},\ \hat{\mathbf{H}} = \sqrt{\mu}\mathbf{H},\ \hat{\mathbf{J}} = \sqrt{\mu}\mathbf{J},\ \text{and}\ \hat{\rho} = \frac{1}{\sqrt{\varepsilon}}\rho. \tag{2.17}$$

Substituting these in (2.12)–(2.15) yields a system depending only on the wave-number $\kappa = \omega\sqrt{\varepsilon\mu}$. Moreover, in certain formulations of boundary integral equations, the normalized fields yield more stable numerical systems as the (normalized) electric and magnetic are of same scale [10]. The circumflex is omitted from the normalized field variables whenever it does not cause confusion.

In homogeneous medium and for normalized fields the extended Maxwell's equations are obtained by augmenting the original time-harmonic Maxwell's equations (2.12)–(2.15) with scalar slack fields Φ and Ψ: [14, 10]

$$\left(\begin{bmatrix} 0 & 0 & \nabla\cdot & 0 \\ 0 & 0 & -\nabla\times & \nabla \\ \nabla & \nabla\times & 0 & 0 \\ 0 & \nabla\cdot & 0 & 0 \end{bmatrix} - i\kappa I \right) \begin{bmatrix} \Phi \\ \hat{\mathbf{E}} \\ \hat{\mathbf{H}} \\ \Psi \end{bmatrix} = \begin{bmatrix} 0 \\ -\hat{\mathbf{J}} \\ 0 \\ \hat{\rho} \end{bmatrix}. \tag{2.18}$$

It holds that if $\Phi = \Psi = 0$, then $\hat{\mathbf{E}}$ and $\hat{\mathbf{H}}$ are solutions to Maxwell's equations (2.12)–(2.15). On the other hand, the restriction $\hat{\mathbf{E}} = \Psi = 0$ implies that Φ and $\hat{\mathbf{H}}$ satisfy acoustic time harmonic field equations

$$\begin{cases} \nabla \cdot \hat{\mathbf{H}} - i\kappa\Phi = 0 \\ \nabla\Phi - i\kappa\hat{\mathbf{H}} = 0. \end{cases} \tag{2.19}$$

Thus, the extended Maxwell's equations can be viewed as a combination of electromagnetic and acoustic field equations [13].

The merit of the system (2.18) is that the dimension of the null-space is equal to the sum of its number of connected components, handles and holes (i.e., the the number of connected components of its complement minus one) of the domain in which the equation is posed [13, 12, 6, 15]. For the domain shown in Figure 2.1 the dimension is thus 4. Specifically in simply connected bounded domains $\mathcal{P}$ is an isomorphism from certain natural energy spaces, discussed in Chapter 5, to locally square integrable vector fields.

In this thesis, the system (2.16) is exploited in exterior domains in conjunction with surface integral equations and the PEC boundary condition

$$\mathbf{n} \times \mathbf{E} = 0 \quad \text{on } \partial\Omega \tag{2.20}$$

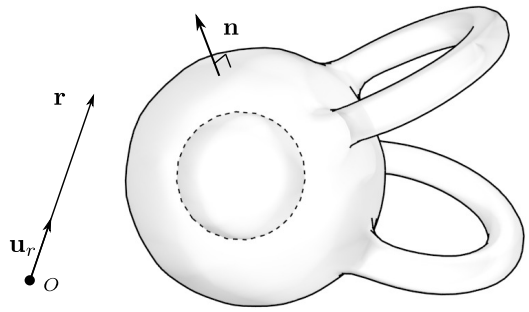

Figure 2.1. A boundary of a domain Ω in $\mathbb{R}^3$ with 2 handles and 1 hole (dotted line). The exterior normal of Ω is denoted with $\mathbf{n}$. The position vector is denoted by $\mathbf{r}$ and its length r the radial distance from origin O. The unit radial vector is $\mathbf{u}_r = \mathbf{r}/r$.

and the Silver-Müller radiation condition [16, 17]

$$|\sqrt{\varepsilon}\mathbf{E} - \sqrt{\mu}\mathbf{H} \times \mathbf{u}_r| \leq O(r^{-2}) \quad \text{as } r \to \infty, \tag{2.21}$$

where the unit radial vector $\mathbf{u}_r$ and the position vector $\mathbf{r}$ are displayed in Figure 2.1, and the radial coordinate r is the length of $\mathbf{r}$.

The extended equation (2.18) is analysed in interior domains satisfying the generalized versions of PEC and PMC boundary conditions:

$$\begin{cases} \mathbf{n} \times \hat{\mathbf{E}} = 0,\ \mathbf{n} \cdot \hat{\mathbf{H}} = 0,\ \Psi = 0 \quad \text{(PEC)} \\ \mathbf{n} \times \hat{\mathbf{H}} = 0,\ \mathbf{n} \cdot \hat{\mathbf{E}} = 0,\ \Phi = 0 \quad \text{(PMC)} \end{cases} \quad \text{on } \partial\Omega. \tag{2.22}$$

3. The field problem

The purpose of this chapter is to introduce the prototypical boundary element methods employed in the CEM. To that end, the energy spaces encountered in the CEM are reviewed and finite elements are discussed at large to fix notations. Following that, BEM discretizations of PEC scattering problems are discussed. The scattering problem is transformed to equivalent electric, magnetic and combined field boundary integral equations, which discretized with finite elements and the method of moments lead to linear algebraic equations.

It should be noted that within the CEM community generally any numerical method to solve electromagnetic field problems with integral equations is often referred to as the "Method of Moments" [18] instead of BEM.

3.1 Energy spaces and their traces

Let $\Omega \subset \mathbb{R}^3$ be an open Lipschitz domain [19] with a compact closure. Its exterior is denoted by $\Omega_e = \mathbb{R}^3 \setminus \overline{\Omega}$ and its boundary by $\Gamma = \partial\Omega$. A domain is said to be Lipschitz if it can be described with a graph of a Lipschitz function locally near boundary as follows [19, 20]. A domain Ω is Lipschitz if for every $x_0 \in \partial\Omega$ there is a bounded right open circular cylinder C whose axis $\mathbf{N}$ runs through x_0 and is orthogonal to a plane H containing x_0 so that for some Lipschitz continuous function $\phi : H \to \mathbb{R}$

(a) $\Omega \cap C = C \cap \{x' + t\mathbf{N} : \ x' \in H, \ t > \phi(x')\}$

(b) $\Omega_e \cap C = C \cap \{x' + t\mathbf{N} : \ x \in H, \ t < \phi(x')\}$

(c) $\partial\Omega \cap C = C \cap \{x' + t\mathbf{N} : \ x' \in H, \ t = \phi(x')\}$

Thus Rademacher's theorem (see e.g. [21]) asserts that one can assign a normal vector, denoted by $\mathbf{n}$, to a boundary of a Lipschitz domain almost everywhere.

The (exterior) normal vector $\mathbf{n}_{x_0}$ at $x_0 \in \partial\Omega$ is that unit vector which points outwards from Ω and is in the null space of the derivative of $(x', t) \mapsto (x', \phi(x'))$. When H is the xy -plane and x_0 is the origin the normal vector, in more familiar terms, is the vector $\nu = \pm\frac{\partial[x,y,\phi(x,y)]}{\partial x} \times \frac{\partial[x,y,\phi(x,y)]}{\partial y}$ normalized to have length of 1 and sign chosen so that it points out from Ω. A surface measure σ on $\partial\Omega$ defined as follows: Let $E \subset \partial\Omega$ be an open set contained in $C \cap \partial\Omega$ and $E = \phi(\hat{E})$, then

$$\sigma(E) = \int_{\hat{E}} \|\nu\| d\lambda, \tag{3.1}$$

where λ is the Lebesgue measure on H. When it is not clear with respect to which variable integration is carried on a surface, the measure σ is subscripted with the variable symbol, e.g. $\int_E f(\mathbf{r}, \mathbf{r}') d\sigma_{\mathbf{r}}$ is an expression with $\mathbf{r}'$ being a free variable.

The notion almost everywhere in this context is defined using the cylinder C and the plane H: An assertion $P(x)$ holds almost everywhere near $x_0 \in \partial\Omega$ if the Lebesgue measure of the set $C \cap H \setminus \{x' : P(x' + \mathbf{N}\phi(x')\}$ is zero. However, a surface measure of a set on the boundary vanishes, if and only if the measure of the projection of the set to the corresponding plane H vanishes also. Thus one can utilize the notion "almost everywhere" on a surface without resorting to a particular plane and cylinder.

The following Sobolev spaces play an important role in the CEM as they encode the finite-energy conditions of the electromagnetic fields:

$$\begin{cases} H^1(\Omega) := \{f \in L_2(\Omega) : \|\nabla f\|_{L_2} < \infty\} \\ \mathbf{H}(\nabla\times, \Omega) := \{f \in L_2(\Omega) : \|\nabla \times f\|_{L_2} < \infty\} \\ \mathbf{H}_0(\nabla\times, \Omega) := \{f \in \mathbf{H}(\nabla\times, \Omega) : \mathbf{n} \times f = 0 \text{ on } \Gamma\} \\ \mathbf{H}(\nabla\cdot, \Omega) := \{f \in L_2 : \|\nabla \cdot f\|_{L_2} < \infty\} \\ \mathbf{H}_0(\nabla\cdot, \Omega) := \{f \in \mathbf{H}(\nabla\cdot, \Omega) : \mathbf{n} \cdot f = 0 \text{ on } \Gamma\} \end{cases} \tag{3.2}$$

The symbol Ω is omitted whenever it is clear on which domain the function space is defined. The zero normal and tangential traces appearing in $\mathbf{H}_0(\nabla\cdot)$ and $\mathbf{H}_0(\nabla\times)$ are posed in a distributional sense:

$$\begin{cases} \mathbf{f} \in \mathbf{H}_0(\nabla\cdot; \Omega) & \Leftrightarrow \quad \int_\Omega \nabla \cdot \mathbf{f}\phi + \mathbf{f} \cdot \nabla\phi dx = 0 \quad \forall \phi \in C_0^\infty(\mathbb{R}^3) \\ \mathbf{f} \in \mathbf{H}_0(\nabla\times; \Omega) & \Leftrightarrow \quad \int_\Omega \nabla \times \mathbf{f} \cdot \boldsymbol{\phi} - \mathbf{f} \cdot \nabla \times \boldsymbol{\phi} dx = 0 \quad \forall \boldsymbol{\phi} \in (C_0^\infty(\mathbb{R}^3))^3. \end{cases} \tag{3.3}$$

Other than zero boundary values are usually posed in CEM for electric or magnetic fields, and thus it makes sense to question exactly what kind of boundary values are permitted for the boundary value problem to be solvable.

To that end, let us consider an electrostatic model problem in unit square $Q = (0,1) \times (0,1) \subset \mathbb{R}^2$ with $\Gamma_1 = \{(x,y) \in \partial Q \;\big|\; x = 1\}$ and $\Gamma_2 = \partial Q \setminus \Gamma_1$:

$$\begin{cases} -\Delta\phi = 0 & \text{in } Q \\ \phi_{\big|\Gamma_1} = 1, \quad \phi_{\big|\Gamma_2} = 0 & \text{on } \partial Q. \end{cases} \tag{3.4}$$

This problem has a unique formal series solution as a limit $M \to \infty$ of

$$\phi_M(x,y) = 4 \sum_{m=1}^{M} \frac{\sinh(\pi(2m-1)x)\sin(\pi(2m-1)y)}{\pi(2m-1)\sinh(\pi(2m-1))} \tag{3.5}$$

but $\|\nabla\phi_M\|_{L_2} \to \infty$ as $M \to \infty$. Thus this problem has no finite energy solutions. Moreover, the solution of Laplace equation cannot depend continuously on $g \in L_2(\partial Q)$ in $H^1(\Omega)$.

The remedy is to consider the restriction as an boundary trace operator $\gamma : H^1(Q) \to Y(\partial Q)$, where $Y(\partial Q)$ is a Banach space. It must be such that it coincides with the usual boundary restriction to smooth functions, every function in H^1 must have a boundary trace and every function in $Y(\partial Q)$ must be a boundary trace of some function in H^1, i.e., it must be surjective. The last two properties entail that graph of γ is $H^1(Q) \times Y(\partial Q)$ which is closed and thus γ must be also continuous by closed graph theorem. For basic theory on functional analysis we refer to [22]

Thus, the trace operator must be continuous and surjective, i.e., onto.

Let us in the following again consider the domain Ω and denote the boundary data space $Y(\Gamma)$ by $H^{\frac{1}{2}}(\Gamma)$.

Equipping $H^{\frac{1}{2}}(\Gamma)$ with the Gagliardo norm

$$\|u\|_{H^{\frac{1}{2}}} = \left(\int_\Gamma |u(\mathbf{r})|^2 d\sigma_{\mathbf{r}} + \int_{\Gamma\times\Gamma} \frac{|u(\mathbf{r}) - u(\mathbf{r}')|^2}{|\mathbf{r} - \mathbf{r}'|^3} d\sigma_{\mathbf{r},\mathbf{r}'} \right)^{\frac{1}{2}} \tag{3.6}$$

the boundary trace operator $\gamma : H^1(\Omega) \to H^{\frac{1}{2}}(\Gamma)$ is bounded and surjective [19, 23]. Thus, it is straightforward to define H^1_0 as the kernel of γ and $\mathbf{n}\cdot$ by duality as a continuous surjective operator $\mathbf{H}(\nabla\cdot, \Omega) \to H^{-\frac{1}{2}}(\Gamma)$, where $H^{-\frac{1}{2}}(\Gamma)$ is the dual space of $H^{\frac{1}{2}}(\Gamma)$ having $L_2(\Gamma)$ as the pivot space [24].

The above characterisation of $\gamma H^1(\Omega)$ for Lipschitz domains were known as early as the late 1950's due Gagliardo [23]. Girault and Raviart report in their book [24] the properties of $\mathbf{n}\cdot : \mathbf{H}(\nabla\cdot, \Omega) \to H^{-\frac{1}{2}}(\Gamma)$ with a very simple proof.

However, useful characterisations of the trace mapping $\mathbf{n}\times$ on $\mathbf{H}(\nabla\times, \Omega)$ attributed to Tartar [25] and further developed by Buffa et al [26, 27] were only understood in the early 2000's. Thus it took almost 50 years for the trace space characterisations to mature for the use of computational

electromagnetics. In the following, results discovered by Buffa et al in [26, 27] are reviewed.

If Ω has a piecewise smooth boundary, which is often the case in numerical simulations, the trace space of $\mathbf{n}\times$ has the following characterisation:

Define $\mathbf{H}_{||}^{-\frac{1}{2}}(\nabla_\Gamma\cdot;\Gamma)$ as

$$\mathbf{H}_{||}^{-\frac{1}{2}}(\nabla_\Gamma\cdot;\Gamma)=\left\{u\in\mathbf{H}_{||}^{-\frac{1}{2}}:\ \nabla_\Gamma\cdot u\in H^{-\frac{1}{2}}\right\}, \tag{3.7}$$

where $\mathbf{H}_{||}^{-\frac{1}{2}}(\Gamma)$ is the dual space of $\mathbf{n}\times\mathbf{n}\times\mathbf{H}^1(\Omega)=\mathbf{H}_{||}^{\frac{1}{2}}$ with tangential $\mathbf{L}_2$ as pivot space. The space $\mathbf{H}_{||}^{\frac{1}{2}}$ is defined to be the range of $\mathbf{n}\times\mathbf{n}\times\mathbf{H}^{\frac{1}{2}}(\Gamma)$ as a subspace of $\mathbf{L_t}(\mathbf{\Gamma})$ and it is equipped with a norm that makes $\mathbf{n}\times\mathbf{n}\times$ automatically bounded; the norm of $\mathbf{v}$ in $\mathbf{n}\times\mathbf{n}\times\mathbf{H}^{\frac{1}{2}}(\mathbf{\Gamma})$ is

$$\inf_{\substack{\mathbf{u}\in\mathbf{H}^{\frac{1}{2}}(\mathbf{\Gamma})\\ \mathbf{v}=\mathbf{n}\times\mathbf{n}\times\mathbf{u}}}\|\mathbf{u}\|_{\mathbf{H}^{\frac{1}{2}}(\mathbf{\Gamma})}. \tag{3.8}$$

It should be noted that the kernel of $\mathbf{n}\times\mathbf{n}\times:\mathbf{H}^{\frac{1}{2}}\to\mathbf{n}\times\mathbf{n}\times\mathbf{H}^{\frac{1}{2}}$ is closed and thus the above formula defines a norm instead of just a seminorm.

For piecewise smooth boundaries, the tangential component trace space $\mathbf{H}_{||}^{\frac{1}{2}}$ has a face-by-face characterisation as a tangential $\mathbf{H}^{\frac{1}{2}}(\Gamma_i)$ for each smooth face Γ_i of Γ with certain weak tangential continuity across the edges of the polyhedron [26]. The surface divergence $\nabla_\Gamma\cdot:\mathbf{H}_{||}^{-\frac{1}{2}}(\Gamma)\to H^{-\frac{3}{2}}(\Gamma)$ is the adjoint-operator of the tangential gradient operator $\nabla_\Gamma:H^{\frac{3}{2}}(\Gamma)\to\mathbf{H}_{||}^{\frac{1}{2}}(\Gamma)$ and $H^{\frac{3}{2}}$ is the trace space of $H^2(\Omega)$ [27]. Furthermore, if $\mathbf{u}=\mathbf{n}\times\mathbf{f}$, where $\mathbf{f}\in\mathbf{H}(\nabla\times;\mathbf{\Omega})$, then $\nabla_\Gamma\cdot\mathbf{u}\in H^{-\frac{1}{2}}(\Gamma)$ by the following reasoning: If $\phi\in C^\infty(\Omega)$, then

$$\begin{aligned}\langle\nabla_\Gamma\cdot\mathbf{u},\phi\rangle&=\langle\mathbf{u},\mathbf{n}\times\mathbf{n}\times\nabla_{\mathbf{\Gamma}}\phi\rangle=\langle\mathbf{n}\times\mathbf{f},\mathbf{n}\times\mathbf{n}\times\nabla_{\mathbf{\Gamma}}\phi\rangle\\&=\int_\Omega\nabla\times\mathbf{f}\cdot\nabla\phi\mathbf{dx}=\int_{\mathbf{\Omega}}\nabla\cdot(\phi\nabla\times\mathbf{f})\mathbf{dx}\le\|\phi\|_{\mathbf{H^1}}\|\mathbf{f}\|_{\mathbf{H}(\nabla\times)}.\end{aligned} \tag{3.9}$$

thus $\nabla_\Gamma\cdot\mathbf{u}$ is continuous linear functional of H^1 and it depends only on scalar boundary traces of H^1.

It holds that

$$\mathbf{n}\times:\mathbf{H}(\nabla\times,\Omega)\to\mathbf{H}_{||}^{-\frac{1}{2}}(\nabla_\Gamma\cdot;\Gamma) \tag{3.10}$$

is continuous and surjective [26].

The trace space of $\mathbf{H}(\nabla\times)$ is considerably more involved than that of $\mathbf{H}(\nabla\cdot)$ because $\mathbf{n}\cdot\mathbf{H}(\nabla\cdot)$ can be characterized as the dual space of $H^{\frac{1}{2}}$ using Green's formula, whereas for $\nabla\times$-operator it yields an antisymmetric bilinear form on $\mathbf{H}(\nabla\times)\times\mathbf{H}(\nabla\times)$. Another obstacle in the construction

of the trace space for a non-smooth domain is that $\mathbf{n}$ is only in $L_\infty(\Gamma)$; if the boundary were smooth one could utilize the smooth sections of tangent bundle of Γ in the construction as multiplication with $\mathbf{n}\times$ would be continuous operation in any Sobolev space on Γ.

In order to complete the picture on trace spaces of $\mathbf{H}(\nabla\times,\Omega)$, we need to consider the tangential component trace operator $\boldsymbol{\pi}$ on $\mathbf{H}(\nabla\times,\Omega)$, defined for smooth fields $\boldsymbol{F}$ by $\boldsymbol{\pi}\boldsymbol{F} = -\mathbf{n}\times(\mathbf{n}\times\boldsymbol{F})$. Characterisation of the target space of $\boldsymbol{\pi}$ allows us to make sense of the elementary integration by parts formula

$$\int_\Omega \nabla\times\mathbf{u}\cdot\mathbf{v} - \mathbf{u}\cdot\nabla\times\mathbf{v}dx = \int_\Gamma \mathbf{n}\times\mathbf{u}\cdot\boldsymbol{\pi}\mathbf{v}d\sigma_x. \tag{3.11}$$

The trace space for which $\boldsymbol{\pi}$ is continuous, surjective and satisfies (3.11) is, roughly speaking, the rotated version of $\mathbf{H}_{||}^{-\frac{1}{2}}(\nabla_\Gamma\cdot;\Gamma)$:

The mapping

$$\boldsymbol{\pi} : \mathbf{H}(\nabla\times,\Omega) \to \mathbf{H}_{\perp}^{-\frac{1}{2}}(\nabla_\Gamma\times;\Gamma) \tag{3.12}$$

is continuous, surjective and it satisfies (3.11) [26]. Furthermore, $\mathbf{H}_{||}^{-\frac{1}{2}}(\nabla_\Gamma\cdot;\Gamma)$ and $\mathbf{H}_{\perp}^{-\frac{1}{2}}(\nabla_\Gamma\times;\Gamma)$ are isomorphic and the isomorphism restricted to traces of smooth fields is just rotation around the normal vector by 90 degrees [27].

3.2 Finite elements

Finite elements are useful in systematising approximations in Sobolev spaces. They rest on partitioning the geometry of the domain into non-overlapping open elementary geometrical domains so that on each domain the approximation has a closed form expression that is straightforward to evaluate.

More precisely, a finite element in the sense of Ciarlet [28] is a triple $\mathcal{E} = (T, V, \Sigma)$, where

(i) T is an open geometric domain,

(ii) V is a finite dimensional function space on T and

(iii) $\Sigma \subset V'$, i.e. Σ is a set of linear functionals on T. They are called the degrees of freedom.

Usually T is a triangle or quadrilateral in two dimensions and a tetrahedron or hexahedron in three dimensions, V is a set of polynomials on T and Σ is a set of point evalations on T. It is useful to choose the functionals Σ so that the element is *unisolvent* [29]: If $v_1,\ldots,v_n$ span V and

$\Sigma = (\sigma_1, \ldots, \sigma_m)$, then the element E is unisolvent if the matrix $A_{ij} = \sigma_i(v_j)$ is square and non-singular.

Let now $(T^j)_{j=1}^M$ be a partition of $\Omega \subset \mathbb{R}^2$ to M triangles then the elements $(T^j, V^j, \Sigma^J)_j$ provide a *finite element* space S_M by

$$S_M = \operatorname*{span}_{v_i^j \in V^j} v_i^j. \tag{3.13}$$

Such FE spaces are only subspaces of integrable functions because they are spanned by piecewise polynomial functions. However, imposing constraints to the degrees of freedom across elements yield more regular FE spaces. For example when V^j consists of first order polynomials and Σ^j of point evaluations at vertices of T^j, requiring that $\sigma_{i_1}^{j_1}(v_k^{j_1}) = \sigma_{i_2}^{j_2}(v_l^{j_2})$ for all $l, k = 1, 2, 3$, if $\sigma_{i_1}^{j_1}$ and $\sigma_{i_2}^{j_2}$ are associated to a same point in Ω, yields the first order nodal Lagrange finite element space.

If, for arbitrary indices i, j, T_i and T_j can be mapped affinely (or diffeomorphically) to each other, it is useful to define single reference element $\hat{\mathcal{E}}$ so that for given T_i in the partition there is an affine (diffeomorphic) map F_{T_i} and a reference domain $\hat{T}$ s.t. $T_i = F_{T_i}\hat{T}$. The induced mapping that takes functions from $\hat{V}$ to V_i depends on the element, however. For scalar Lagrange interpolating elements it is just the pullback $F_{T_i}^* V_i = \hat{V}$, i.e., for given $\hat{\lambda} \in \hat{V}$, corresponding $\lambda \in V_i$ is given by $F_{T_i}^* \lambda(x) = \lambda(F_{T_i}(x)) = \hat{\lambda}(x)$.

Popular finite elements in CEM are the Nédélec elements [30], Raviart-Thomas elements [31], rediscovered in the method of moments setting by Rao, Wilton and Glisson [32], and the nodal Lagrange elements [33, 34].

Let us elucidate the equivalence of the RT and RWG elements in the following.

Let two triangles K and L share an edge $\mathbf{e}$ and denote the vertices of K and L opposite to $\mathbf{e}$ by p_K and p_L, respectively. The RWG function associated with $\mathbf{e}$ is then given by

$$\mathbf{u}(x) = \begin{cases} \frac{|\mathbf{e}|}{2|K|}\,(x - p_K) & x \in K \\ -\frac{|\mathbf{e}|}{2|L|}\,(x - p_L) & x \in L \end{cases} \tag{3.14}$$

where $|K|$ is the area of K (resp. $|L|$) and $|\mathbf{e}|$ is the length of $\mathbf{e}$.

The degrees of freedom are given by $\mathbf{n} \times \mathbf{u}(x_\mathbf{e}) \cdot \frac{\mathbf{e}}{|\mathbf{e}|}$, where $\mathbf{n}$ is the exterior normal of K or L and $x_\mathbf{e}$ is the centre point of $\mathbf{e}$. The factor $|\mathbf{e}|$ may be omitted from (3.14), in which case the restriction $\mathbf{u}\big|_K$ can be constructed with a reference element and the Piola transformation (see e.g. [33]) as follows.

The reference domain is the unit 2-simplex

$$\hat{K} = \{\xi, \eta \in \mathbb{R} : \, 0 < \xi, \eta \text{ and } \xi + \eta < 1\}, \tag{3.15}$$

the reference basis functions on $\hat{K}$ are $[\xi, \eta]$, $[\xi, 1-\eta]$, and $[1-\xi, \eta]$ and the mapping that takes the basis functions from the reference triangle to K is the Piola transformation: Let $\hat{\mathbf{u}}$ be smooth tangent field of $\hat{K}$, then the Piola transformation $\mathcal{P}_F\hat{\mathbf{u}}$ of $\hat{\mathbf{u}}$ is the unique tangent field of K which satisfies

$$(\mathcal{P}_F\hat{\mathbf{u}}) \circ F = \frac{1}{\sqrt{g_{ij}}} F'\hat{\mathbf{u}} \tag{3.16}$$

where F' is the the Jacobian of the map $F : \hat{K} \to K$ and $\sqrt{g_{ij}}$ is the square root of the determinant of the metric tensor on K in (ξ, η)-coordinates. If K is flat, then $\sqrt{g_{ij}} = 2|K|$ and thus it holds that there is one-to-one correspondence with RT and RWG functions.

Denoting the nodes of K with $\mathbf{p_1}, \mathbf{p_2}, \mathbf{p_3}$ the mapping F is given by

$$F(\xi, \eta) = (1 - \xi - \eta)\mathbf{p_1} + \xi\mathbf{p_2} + \eta\mathbf{p_3}. \tag{3.17}$$

The important property of the Piola transform is that it gives us a simple formula to calculate the surface divergence on K:

$$(\nabla_K \cdot \mathcal{P}_F\hat{\mathbf{u}}) \circ F = \frac{1}{\sqrt{g_{ij}}} \nabla \cdot \hat{\mathbf{u}}, \tag{3.18}$$

where $\nabla_K \cdot$ is the surface divergence on K and $\nabla \cdot$ is the usual divergence in the Euclidean 2-space. Thus, given a smooth tangential surface vector field if we find a corresponding vector field in Euclidean 2-space through the Piola transform, the calculation of the surface divergence simplifies to the calculation of a divergence in the Euclidean space.

3.3 Boundary integral equations

In a homogeneous medium, the reduced time-harmonic system (2.16) endowed with the Silver-Müller radiation condition (2.21) admits a unique fundamental solution (see e.g. [17]) given by

$$\begin{cases} \mathbf{E} = \left(i\omega\mu - \frac{1}{i\omega\varepsilon}\nabla\nabla\cdot\right)\mathcal{S}_V(\mathbf{J}) + \nabla \times \mathcal{S}_V(\mathbf{M}) \\ \mathbf{H} = \nabla \times \mathcal{S}_V(\mathbf{J}) + \left(-i\omega\varepsilon + \frac{1}{i\omega\mu}\nabla\nabla\cdot\right)\mathcal{S}_V(\mathbf{M}) \end{cases} \tag{3.19}$$

where $\mathcal{S}_V$ is the potential operator

$$(\mathcal{S}_V v)(\mathbf{r}) = (G * v)(\mathbf{r}), \tag{3.20}$$

with $G(\mathbf{r}) = \frac{e^{ik|\mathbf{r}|}}{4\pi|\mathbf{r}|}$ being the fundamental solution of the Helmholtz equation: $-(\Delta + k^2)G = \delta$. If a distribution $v \in \mathcal{E}'$ is a product of δ_Γ and some sufficiently smooth function f, the convolution results in the single layer potential $\mathcal{S}f$:

$$(\mathcal{S}f)(\mathbf{r}) = \int_\Gamma G(\mathbf{r} - \mathbf{r}')f(\mathbf{r}')d\sigma_{\mathbf{r}'}. \tag{3.21}$$

The two kinds of integro-differential operators appearing in (3.19) are defined by

$$\begin{cases} \mathcal{T}_V(\mathbf{v}) = (k^2 + \nabla\nabla\cdot)\mathcal{S}_V(\mathbf{v}), \\ \mathcal{K}_V(\mathbf{v}) = \nabla \times \mathcal{S}_V(\mathbf{v}). \end{cases} \tag{3.22}$$

Again, if $\mathbf{v} = \delta_\Gamma \mathbf{F}$ with smooth $\mathbf{F}$ the convolutions above result in boundary integrals

$$\begin{cases} \mathcal{T}(\mathbf{F}) = (k^2 + \nabla\nabla\cdot)\mathcal{S}(\mathbf{F}) \\ \mathcal{K}(\mathbf{F}) = \nabla \times \mathcal{S}(\mathbf{F}). \end{cases} \tag{3.23}$$

Let $\Omega \subset \mathbb{R}^3$ be a bounded domain with sufficiently regular boundary or an exterior of such a domain. Furthermore, let us suppose that $\mathbf{E}$ and $\mathbf{H}$ satisfy the system (2.16) without source terms $\mathbf{J}$ and $\mathbf{M}$ in an open set strictly containing Ω. Then the following *Stratton-Chu* [35] representation formula holds:

$$\chi_\Omega \begin{bmatrix} \mathbf{E} \\ \mathbf{H} \end{bmatrix} = - \begin{bmatrix} -\frac{1}{i\omega\varepsilon}\mathcal{T} & \mathcal{K} \\ \mathcal{K} & \frac{1}{i\omega\mu}\mathcal{T} \end{bmatrix} \begin{bmatrix} \mathbf{n} \times \mathbf{H} \\ -\mathbf{n} \times \mathbf{E} \end{bmatrix}, \quad \text{in } \mathbb{R}^3 \setminus (\partial\Omega \cup R)\,. \tag{3.24}$$

Here χ_Ω is the indicator function of Ω, R is the smallest closed set containing the sources and $\mathbf{n}$ is the exterior normal of Ω.

The tangential traces of the representation formula (3.24) are the basis for most of the surface integral equations in electromagnetics [17, 32, 36, 18].

To that end, let $\mathbf{v}$ be a square-integrable vector field having square-integrable surface divergence on a Lipschitz surface Γ whose normal component vanishes almost everywhere. Then, the following limit formulas hold a.e. $\mathbf{r} \in \Gamma$ [37]:

$$\mathbf{n} \times \mathcal{K}(\mathbf{v})(\mathbf{r}^\pm) = \pm\frac{1}{2}\mathbf{v} + \mathbf{n} \times \left(p.v. \nabla \times \int_\Gamma G(\mathbf{r} - \mathbf{r}')\mathbf{v}(\mathbf{r}')d\mathbf{r}' \right) \tag{3.25}$$

and

$$\begin{aligned} \mathbf{n} \times \mathcal{T}(\mathbf{v})(\mathbf{r}^\pm) = \mathbf{n} \times \Bigg(& k^2 \int_\Gamma G(\mathbf{r} - \mathbf{r}')\mathbf{v}(\mathbf{r}')d\mathbf{r}' \\ & + p.v. \nabla_\Gamma \int_\Gamma G(\mathbf{r} - \mathbf{r}')\nabla_\Gamma \cdot \mathbf{v}(\mathbf{r}')d\mathbf{r}' \Bigg)\,. \end{aligned} \tag{3.26}$$

Here $\mathbf{r}^+$ and $\mathbf{r}^-$ denote the exterior and interior normal limits, respectively, defined by

$$f(\mathbf{r}^{\pm}) = \lim_{h \downarrow 0} f(\mathbf{r} \pm h\mathbf{n}). \tag{3.27}$$

The principal value integral $p.v.$ is defined by

$$p.v. \int G(\mathbf{r} - \mathbf{r}')f(\mathbf{r}')d\mathbf{r}' = \lim_{\epsilon \downarrow 0} \int_{\|\mathbf{r}-\mathbf{r}'\|>\epsilon} G(\mathbf{r} - \mathbf{r}')f(\mathbf{r}')d\mathbf{r}'. \tag{3.28}$$

In fact, the normal limits may be substituted with non-tangential ones, where the limit is taken, roughly speaking, in an open cone contained in Ω or Ω_e having vertex at $\mathbf{r} \in \Gamma$. However, the construction is highly technical and therefore omitted, for reference, see [38, 37].

The operators on the right hand side can be extended to bounded operators from $\mathbf{H}_{||}^{-\frac{1}{2}}(\nabla_\Gamma \cdot; \Gamma)$ to itself when Γ is a piecewise smooth Lipschitz polyhedron [26]. These extensions are denoted by

$$K(\mathbf{v})(\mathbf{r}) = \mathbf{n} \times \left(p.v. \nabla \times \int_\Gamma G(\mathbf{r} - \mathbf{r}')\mathbf{v}(\mathbf{r}')d\mathbf{r}' \right) \tag{3.29}$$

and

$$\begin{aligned} T(\mathbf{v})(\mathbf{r}) = \mathbf{n} \times \Bigg(& k^2 \int_\Gamma G(\mathbf{r} - \mathbf{r}')\mathbf{v}(\mathbf{r}')d\mathbf{r}' \\ & + p.v. \nabla_\Gamma \int_\Gamma G(\mathbf{r} - \mathbf{r}')\nabla_\Gamma \cdot \mathbf{v}(\mathbf{r}')d\mathbf{r}' \Bigg). \end{aligned} \tag{3.30}$$

These operators give rise to the following representation theorem for the scattering problem: Suppose that $\mathbf{H}^s$ and $\mathbf{E}^s$ are scattered fields having fictitious sources in Ω, and $\mathbf{H}^p$ and $\mathbf{E}^p$ are primary fields whose sources lie at a positive distance away from Ω. Then it holds that

$$\begin{bmatrix} \mathbf{n} \times \mathbf{E}^p \\ \mathbf{n} \times \mathbf{H}^p \end{bmatrix} = \begin{bmatrix} \frac{1}{i\omega\varepsilon} T & \frac{1}{2} I - K \\ \frac{1}{2} I - K & \frac{1}{i\omega\mu} T \end{bmatrix} \begin{bmatrix} \mathbf{j} \\ \mathbf{m} \end{bmatrix}, \tag{3.31}$$

where $\mathbf{j} = \mathbf{n} \times \mathbf{H}$ and $\mathbf{m} = -\mathbf{n} \times \mathbf{E}$ are the electric and magnetic surface currents, respectively.

By plugging in the PEC boundary condition $\mathbf{n} \times \mathbf{E} = 0$ to the above equation, the EFIE and MFIE [39, 36] given by

$$\begin{cases} \mathbf{n} \times \mathbf{E}^p = \frac{1}{i\omega\varepsilon} T(\mathbf{j}) & \textbf{(EFIE)} \\ \mathbf{n} \times \mathbf{H}^p = \left(\frac{1}{2} I - K \right)(\mathbf{j}) & \textbf{(MFIE)} \end{cases} \tag{3.32}$$

are obtained.

At certain interior resonance frequencies the operators on the right hand side fail to be injective [40]. However, the following linear combination of

above equations, known as the CFIE, is injective for all non-zero frequencies [41, 40, 39]:

$$\alpha \mathbf{n} \times \mathbf{E}^p - (1-\alpha)\eta \mathbf{n} \times \mathbf{n} \times \mathbf{H}^p = \frac{\alpha}{i\omega\varepsilon} T(\mathbf{j}) - (1-\alpha)\eta \mathbf{n} \times (\frac{1}{2} - K)(\mathbf{j}), \quad (3.33)$$

where $0 < \alpha < 1$ and $\eta = \sqrt{\mu/\varepsilon}$ is the wave impedance of the medium.

Indeed, this formulation has been successfully applied to very large scale scattering problems [42, 43], regardless of the summation between elements in two different spaces, namely $\mathbf{H}_{||}^{-\frac{1}{2}}(\nabla_\Gamma \cdot; \Gamma)$ and $\mathbf{H}_{\perp}^{-\frac{1}{2}}(\nabla_\Gamma \times; \Gamma)$. The proper way to discretize and derive the CFIE equations have been, however, under active research in the recent years. The most promising approach to discretize the MFIE part, reported in [44], exploits basis functions described in [45]. These Buffa-Christiansen (BC) basis functions suit in certain preconditioning schemes of the EFIE [46] and have been used in CFIE type formulations for impedance boundary conditions where the primary electric and rotated magnetic field are linearly related through surface impedance [47]. In [48] the summtion of the CFIE is performed in the space $\mathbf{H}_{||}^{-\frac{1}{2}}(\nabla_\Gamma \cdot; \Gamma)$ and the discretization, again, utilizes the BC basis functions.

The discrete EFIE is obtained in a weak sense with the aid of the bilinear antisymmetric mapping

$$\langle \mathbf{u}, \mathbf{v} \rangle_\times = \int_\Gamma \mathbf{n} \times \mathbf{u} \cdot \mathbf{v} d\sigma, \quad (3.34)$$

which extends to an antisymmetric duality pairing on $\mathbf{H}_{||}^{-\frac{1}{2}}(\nabla_\Gamma \cdot; \Gamma)$ [49]. Thus, the weak form of the EFIE is given by:

$$\begin{aligned} &\text{Find } \mathbf{j} \in \mathbf{H}_{||}^{-\frac{1}{2}}(\nabla_\Gamma \cdot; \Gamma) \text{ s.t.} \\ &\langle \mathbf{v}, \mathbf{n} \times \mathbf{E}^p \rangle_\times = -i\omega\mu \langle \mathbf{v}, \mathbf{n} \times \mathcal{S}\mathbf{j} \rangle_\times - \\ &\qquad \frac{1}{i\omega\varepsilon} \langle \mathbf{v}, \mathbf{n} \times \nabla \mathcal{S} \nabla_\Gamma \cdot \mathbf{j} \rangle_\times, \quad \forall \mathbf{v} \in \mathbf{H}_{||}^{-\frac{1}{2}}(\nabla_\Gamma \cdot; \Gamma). \end{aligned} \quad (3.35)$$

Discretizing this with the RT basis and trial functions yields the following system of equations:

$$\begin{aligned} &\text{Find } \mathbf{j} \in \mathcal{RT}(\Gamma) \text{ s.t.} \\ &\int_\Gamma \mathbf{v} \cdot \mathbf{E}^p d\sigma = -i\omega\mu \int_\Gamma \mathbf{v} \cdot \mathcal{S}(\mathbf{j}) d\sigma - \frac{1}{i\omega\varepsilon} \int_\Gamma \nabla_\Gamma \cdot \mathbf{v} \mathcal{S}(\nabla_\Gamma \cdot \mathbf{j}) d\sigma \quad \forall \mathbf{v} \in \mathcal{RT}(\Gamma). \end{aligned} \quad (3.36)$$

In the RT basis, denoted with $(\boldsymbol{\psi}_1, \ldots, \boldsymbol{\psi}_N)$, this is equivalent with

$$\begin{bmatrix} a(\boldsymbol{\psi}_1, \boldsymbol{\psi}_1) & a(\boldsymbol{\psi}_1, \boldsymbol{\psi}_2) & \ldots & a(\boldsymbol{\psi}_1, \boldsymbol{\psi}_N) \\ a(\boldsymbol{\psi}_2, \boldsymbol{\psi}_1) & a(\boldsymbol{\psi}_2, \boldsymbol{\psi}_2) & & \vdots \\ \vdots & & \ddots & \vdots \\ a(\boldsymbol{\psi}_N, \boldsymbol{\psi}_1) & \ldots & \ldots & a(\boldsymbol{\psi}_N, \boldsymbol{\psi}_N) \end{bmatrix} \begin{bmatrix} \alpha_1 \\ \alpha_2 \\ \vdots \\ \alpha_N \end{bmatrix} = \begin{bmatrix} \int_\Gamma \boldsymbol{\psi}_1 \cdot \mathbf{E}^p d\sigma \\ \int_\Gamma \boldsymbol{\psi}_2 \cdot \mathbf{E}^p d\sigma \\ \vdots \\ \int_\Gamma \boldsymbol{\psi}_N \cdot \mathbf{E}^p d\sigma \end{bmatrix}, \tag{3.37}$$

where

$$a(\boldsymbol{\psi}_m, \boldsymbol{\psi}_n) = -i\omega\mu \int_\Gamma \boldsymbol{\psi}_m \cdot \mathcal{S}(\boldsymbol{\psi}_n) d\sigma - \frac{1}{i\omega\varepsilon} \int_\Gamma \nabla_\Gamma \cdot \boldsymbol{\psi}_m \mathcal{S}(\nabla_\Gamma \cdot \boldsymbol{\psi}_n) d\sigma \tag{3.38}$$

and $\mathbf{j} = \sum_{n=1}^N \alpha_n \boldsymbol{\psi}_n$. In the language of the MoM the coefficients α_n are called moments. This discretization is analysed in [50].

3.4 Fast computation of application of system matrix in boundary integral equations

A major drawback of the BEM is that the arising linear system of equations is dense, making the memory consumption of the method scale quadratically with respect to degrees of freedom, i.e., dimension of the finite element space, denoted by N. Such problems can be solved approximatively with Krylov subspace methods if the matrix-vector product can be calculated sufficiently fast. Such dense products appearing in BEM that involve Helmholtz fundamental solutions, whose direct implementations are of complexity $O(N^2)$, admit however accelerations based on the *fast multipole method* making the Krylov subspace methods feasible.

The idea in the FMM acceleration is in partitioning the system matrix $\mathbf{A}$ into far and near interactions, $\mathbf{A}^{\text{far}}$ and $\mathbf{A}^{\text{near}}$, respectively, so that the number of non-zero entries of $\mathbf{A}^{\text{near}}$ is $O(N)$ and $\mathbf{A}^{\text{far}}$ can be multiplied with a vector faster than in $O(N^2)$ time. This section is devoted to a brief qualitative review of fast multipole methods discussed in, e.g., [51, 52, 53, 54, 55] which significantly accelerate the application of $\mathbf{A}^{\text{far}}$. To that end, let us denote the partition of $(1, \ldots, N)^2$ to near and far interactions by $\mathbf{I}^{\text{near}}$ and $\mathbf{I}^{\text{far}}$, respectively, so that $\mathbf{A}^{\text{near}}_{ij} = \mathbf{A}_{ij}$ whenever $(i,j) \in \mathbf{I}^{\text{near}}$ and 0 otherwise, $\mathbf{A}^{\text{far}} = \mathbf{A} - \mathbf{A}^{\text{near}}$ and $(i,j) \in \mathbf{I}^{\text{far}}$ if and only if $(i,j) \notin \mathbf{I}^{\text{near}}$. Furthermore, for some $D < \infty$ the index set $\mathbf{I}^{\text{near}}$ must satisfy that $(i,j) \notin \mathbf{I}^{\text{near}}$ if $\operatorname{dist}(\operatorname{spt} \boldsymbol{\psi}_i, \operatorname{spt} \boldsymbol{\psi}_j) > D$. Thus the number of non-zero entries in $\mathbf{A}^{\text{near}}$ is $O(N)$.

The high frequency fast multipole methods are based on the Rokhlin's

translation function [51, 52]:

$$T_L(\vec{D},\hat{\boldsymbol{k}}) = \frac{ik}{4\pi}\sum_{n=0}^{L} i^n(2n+1)\, h_n^{(1)}(k|\vec{D}|)P_n\left(\frac{\vec{D}}{|\vec{D}|}\cdot\hat{\boldsymbol{k}}\right) \tag{3.39}$$

It elicits the following approximation of the Green's function:

$$\frac{e^{ik|\vec{D}+\vec{Q}|}}{4\pi|\vec{D}+\vec{Q}|} = \lim_{L\to\infty}\int_{\mathbb{S}_2} e^{ik\vec{Q}\cdot\hat{\boldsymbol{k}}}T_L(\vec{D},\hat{\boldsymbol{k}})d\sigma_{\hat{\boldsymbol{k}}} \tag{3.40}$$

The Rokhlin's translation function arises from the Gegenbauer series of the spherical Hankel function $h_0^{(1)}(x) = \frac{e^{ix}}{ix}$ [56] and the plane-wave expansions of the spherical Bessel functions and the Legendre polynomials [51]. The Gegenbauer series converges uniformly and absolutely when $|\vec{D}| > |\vec{Q}|$ [55, 57] and the truncation error of the limit (3.40) can be controlled by choosing L according to the following empirical *excess bandwidth formula* [53]

$$L \geq k|\vec{Q}| + 1.8d_0^{\frac{2}{3}}(k|\vec{Q}|)^{\frac{1}{3}}, \tag{3.41}$$

where d_0 is the number of significant digits requested from the approximation. In [57] the truncation error is analysed more carefully and in [58] exact values of L are tabulated in a certain configurations of $\vec{Q}$ and $\vec{D}$ appearing in realistic calculations.

Now if $\mathbf{P}_1+\vec{p}$ and $\mathbf{P}_2+\vec{q}$ are in cubes Q_1 and Q_2 so that $\mathbf{r}-\mathbf{r}' = \vec{D}+\vec{p}-\vec{q}$ where $\vec{D} = \mathbf{P}_2-\mathbf{P}_1$, as displayed in Figure 3.1, it holds that

$$\frac{e^{ik|\mathbf{r}-\mathbf{r}'|}}{4\pi|\mathbf{r}-\mathbf{r}'|} \approx \int_{\mathbb{S}_2} e^{ik\vec{p}\cdot\hat{\boldsymbol{k}}}e^{-ik\vec{q}\cdot\hat{\boldsymbol{k}}}T_L(\vec{D},\hat{\boldsymbol{k}})d\sigma_{\hat{\boldsymbol{k}}}. \tag{3.42}$$

This seems an overly complicated way to evaluate Helmholtz's fundamental solution, but its efficiency results in collecting interactions of basis functions contained in larger groups to interactions between the groups themselves. Usually the groups are associated with cubes in $\mathbb{R}^3$ or squares in $\mathbb{R}^2$.

Let us denote the index sets I and J, $I\times J \subset \mathbf{I}^{\text{far}}$, of basis functions $(\boldsymbol{\psi}_m)_{m\in I}$ and $(\boldsymbol{\psi}_n)_{n\in J}$ associated with cubes Q_1 and Q_2, respectively. Thus

$$\sum_{m\in I} a(\boldsymbol{\psi}_n,\boldsymbol{\psi}_m)x_m = y_n \quad n\in J, \tag{3.43}$$

where the bilinear form a is that of EFIE defined in (3.38), is well approximated with

$$y_n = \sum_{m\in I}\int_{\mathbb{S}_2}\int_{\Gamma} e^{i\vec{p}\cdot\hat{\boldsymbol{k}}}\,\boldsymbol{\psi}_n(\mathbf{r})d\sigma_{\mathbf{r}}\int_{\Gamma}\mathcal{P}(ik\hat{\boldsymbol{k}})e^{-ik\vec{q}\cdot\mathbf{r}'}\boldsymbol{\psi}_m(\mathbf{r}')d\sigma_{\mathbf{r}'}T_L(\vec{D},\hat{\boldsymbol{k}})d\sigma_{\hat{\boldsymbol{k}}} \tag{3.44}$$

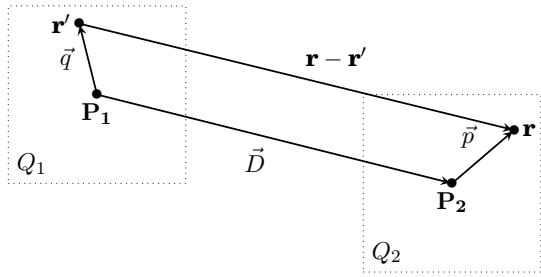

Figure 3.1. The fast multipole picture. Field interactions of the elements in the cube Q_1 and the cube Q_2 can be sparsified with Rokhlin's translation formula to interactions between the cubes.

where $\mathcal{P}$ is a matrix valued polynomial $\mathcal{P}(\boldsymbol{x}) = \frac{1}{i\omega\varepsilon}(k^2 - \boldsymbol{x}\boldsymbol{x}\cdot)$ which for EFIE is chosen such a way that

$$\mathcal{P}(\nabla) = \frac{1}{i\omega\varepsilon}(k^2 - \nabla\nabla\cdot). \tag{3.45}$$

Thus

$$a(\boldsymbol{\psi}_i, \boldsymbol{\psi}_j) = \int_\Gamma \boldsymbol{\psi}_i(\mathbf{r}) \cdot \mathcal{P}(\nabla)(\mathcal{S}\boldsymbol{\psi}_j)(\mathbf{r}) d\sigma_{\mathbf{r}}, \tag{3.46}$$

and by (3.42) it holds that

$$\mathcal{P}(\nabla_{\mathbf{r}})G(\mathbf{r}-\mathbf{r}') \approx \int_{\mathbb{S}_2} \mathcal{P}(ik\hat{\boldsymbol{k}})e^{ik(\vec{p}-\vec{q})\cdot\hat{\boldsymbol{k}}}T_L(\vec{D},\hat{\boldsymbol{k}})d\sigma_{\hat{\boldsymbol{k}}} \tag{3.47}$$

The approximation (3.42) of the Green's function must be numerically integrated over the unit sphere $\mathbb{S}_2$. These two approximations are the source of the error in the fast multipole methods.

In the FMM the surface Γ is covered with cubes $(Q_k)_k$ and the partition $\mathbf{I}^{\text{far}}$ is such that $(i,j) \in \mathbf{I}^{\text{far}}$ if the cubes to which $\boldsymbol{\psi}_i$ and $\boldsymbol{\psi}_j$ are associated do not touch. Thus there are $O(M^2)$ cube to cube interactions instead of $O(N^2)$ basis function to basis function interactions and, moreover, the size of the cubes can be optimized so that the FMM accelerated matrix-vector product scales as $O(N^{\frac{3}{2}})$ [53].

The asymptotic computational load of the FMM can be improved by enclosing Γ inside a single cube which is recursively divided in to eight sub-cubes until the smallest cubes are of suitable size. Those cubes in the resulting octree structure that do not meet Γ are discarded.

The *far field pattern* integrals

$$\mathbf{F}^{\infty}_{Q_k^l}(\hat{\boldsymbol{k}}, \boldsymbol{\alpha}) = \sum_{\boldsymbol{\psi}_m \in Q_k^l} \int_\Gamma \mathcal{P}(ik\hat{\boldsymbol{k}})e^{ik(\mathbf{r}'-\mathbf{P}_k^l)\cdot\hat{\boldsymbol{k}}}\alpha_m\boldsymbol{\psi}_m(\mathbf{r}')d\sigma_{\mathbf{r}'}, \tag{3.48}$$

where $\boldsymbol{\alpha} = \begin{bmatrix}\alpha_1 & \dots & \alpha_N\end{bmatrix} \in \mathbb{C}^N$, are calculated only on the lowest level and to bigger cubes far field pattern from a lower level is aggregated by

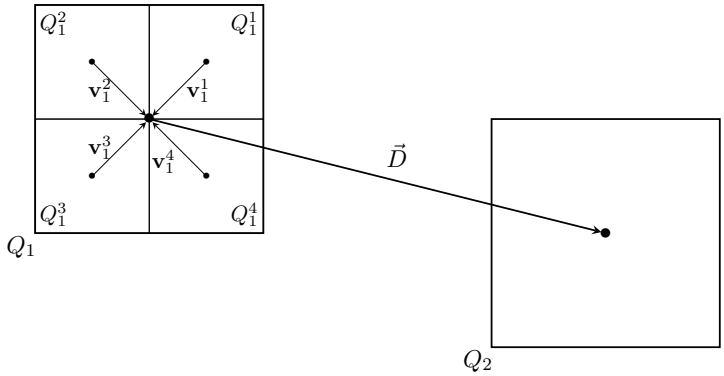

Figure 3.2. In the MLFMA translations are done between larger cubes thus resulting in $O(M)$ translations, where M is the number of cubes. The outgoing field of Q_1 is aggregated from outgoing fields of Q_1^i by interpolation.

multiplying it with an exponential function $e^{ik\mathbf{v}_k^l\cdot\hat{\boldsymbol{k}}}$ where $\mathbf{v}_k^l$, displayed in Figure 3.1, is a vector from the center $\mathbf{P}_k^l$ of lth sub-cube Q_k^l to the center $\mathbf{P}_k$ of Q_k. Thus the far field pattern of Q_k is given by

$$\mathbf{F}_{Q_k}^{\infty}(\hat{\boldsymbol{k}},\boldsymbol{\alpha}) = \sum_{l=1}^{8} e^{ik\mathbf{v}_k^l\cdot\hat{\boldsymbol{k}}}\mathbf{F}_{Q_k^l}^{\infty}(\hat{\boldsymbol{k}},\boldsymbol{\alpha}). \tag{3.49}$$

Finally, the translations between cubes are organized such a way that they are made between maximally large cubes of same size whose closures do not meet. Methods utilizing such multiple levels of cubes are called multilevel fast multipole algorithms (MLFMA) or multilevel fast multipole methods (MLFMM).

The far field patterns $\mathbf{F}_Q^{\infty}(\hat{\boldsymbol{k}},\boldsymbol{\alpha})$ must be sampled at discrete points on $\mathbb{S}_2$ so that the final integral (3.44) is approximated at prescribed accuracy. Furthermore, the aggregation (3.49) must be carried out sufficiently fast and accurately for the algorithm to be efficient because the far field patterns become increasingly oscillatory. The sampling must be the minimal one that yields the requested accuracy at each level. Thus on bigger cubes the sampling becomes denser and the far field patterns from smaller cubes needs to be interpolated to larger cubes. This interpolation is an additional potential source of approximation error of the MLFMA.

The numerical aggregation scheme dictates efficiency of the final MLFMA. In [53] a method based on local interpolators is introduced which makes the MLFMA an $O(N\log N)$ algorithm, where N is the number of degrees

of freedom. A multilevel algorithm based on the FFT reported in [54, 55] achieves $O(N \log^2 N)$ complexity. However, in some cases the local interpolators result in much bigger sample sizes to achieve the same accuracy [54] and, furthermore, both interpolation schemes can be used in a single MLFMA implementation [59]. The development of the interpolators is still an ongoing research topic.

4. Shape optimization and electromagnetics

Ever since there has been efficient algorithms to tackle the electromagnetic scattering problem, there has been interest in the domain problem: find a domain that yields the desired scattering properties. In fact, the domain problem is, at least for an engineer, the reason to solve the field problem in the first place; we wish to design apparatuses that result in desired electromagnetic behaviour. It should be noted that depending on a speaker, this problem could be called an inverse problem, a shape optimization problem or a design problem.

In this chapter different techniques to deal with the shape optimization problem in CEM are outlined. We start with an example design utilizing black-box thinking and then highlight how viewing the problem as a PDE restricted optimization problem results in an efficient gradient optimization method known as the adjoint variable method. Finally, details concerning Publications II and III are presented.

4.1 Yagi-Uda antenna array

Let us consider the Yagi-Uda antenna array [60] design problem where one tries to find optimal directivity in the main direction and input impedance close to some prescribed value. This problem, particularly the directivity part, and its variants have been studied extensively in the literature (c.f. [61, 62, 63, 64, 65, 66], to name a few). Thus it serves as a perfect model problem for shape optimization in CEM.

A Yagi-Uda array consists of a feed dipole, parasitic "Wave reflector" dipole and one to eight "Wave director" dipoles, as phrased by Yagi and Uda [60], parasitic as well. An array with one director dipole is shown in Figure 4.1. The design parameters for Yagi-Uda antennas are spacings $d_1, \ldots, d_n$ and lengths $w_1, \ldots, w_n$ of the elements.

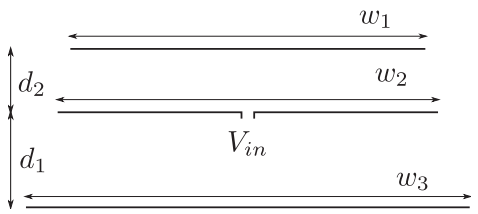

Figure 4.1. Yagi-Uda array optimization problem

Successful strategies to solve this problem in the past include measuring or simulating the antenna gain and impedance for selected spacings and lengths chosen in a smart manner and interpolating the intermediate values resulting in an empirical design formula [66, 63].

A rather simplistic but functional approach to solve this problem is to let a computer program calculate the value of some cost function $\mathcal{J}$ depending on the design variables $d_1, \ldots, d_n, w_1, \ldots, w_n$ and apply a non-linear optimization algorithm to $\mathcal{J}$. If the optimization algorithm requires derivatives of $\mathcal{J}$, they need to be calculated with finite differences.

Using the BFGS (see e.g. [67]) algorithm the values $d_1 = 0.35\lambda$, $d_2 = 0.23\lambda$, $[w_1, w_2, w_3] = [0.452\lambda, 0.468\lambda, 0.4832\lambda]$ are obtained. These parameters yield an antenna with 8.6 dB directivity and input impedance of $44.1 - 0.8i\ \Omega$ when the equivalent radius of the wire, a concept discussed in the Publication I and [68], is $\lambda/2000$.

However, by bending the wire dipoles, considerably higher directivities can be achieved as demonstrated by Landstorfer [69]. Thus, the complete optimization problem would include the shapes of the feed and the parasitic elements as well.

In the Publication I the shapes of the wire dipoles are parametrized such a way computing $\mathcal{J}$ is reliable and the space of possible shapes for the elements is restricted by physical limitations. Thus, the wire dipole shaping process set forth by Landstorfer in [69] is taken to its extreme in a sense that widening the parameter space further would yield antennas that are not wire dipoles.

The black box mindset for computing the value of the cost function works well when the evaluation of $\mathcal{J}$ is relatively cheap so that it is feasible to approximate its gradient with a difference formula. However, an FD approximation of $\nabla\mathcal{J}$ leads to $k + 1$ evaluations of $\mathcal{J}$. This not permissible when the model and the parameter space grows large.

Furthermore, in order for the FD approximation to make sense, the

interior of the parameter space should have some normed vector space structure and it should be equipped with such a topology that reflects the true geometric design: small changes in the parameter space must translate to small changes in the geometry.

Usually, however, the $\mathcal{J}$ is not a black box. instead, in a typical shape optimization scenario $\mathcal{J}$ can be viewed as a function of shape parameters and the solution of *state equation* [70, 3], e.g. surface current of the antenna with given shape parameters.

Antenna optimization problems can be solved using global optimization methods as well. For example genetic algorithms [71, 72] and simulated annealing [73] have been successfully applied in antenna optimization. In [74] one finds a more comprehensive treatment on geometric optimization applied in electromagnetics.

In contrast to gradient based local methods, global optimization methods don't terminate at local optima but they often require considerably more function evaluations. Moreover, if an optimization method does not employ gradient information, such as is the case with the above genetic algorithms or simulated annealing, the solutions it provides are not necessarily critical points, i.e., points where gradient of the objective function vanishes.

However, it is difficult to say if some local method utilizing gradient information, such as the BFGS method, is the best algorithm for antenna shape optimization not only because global optimization is very active field of research[1] but also because the local optimum, which although can be achieved quickly, can be a very bad candidate solution to the design problem.

4.2 PDE restricted shape optimization

Let us briefly formulate an abstract shape optimization problem restricted by a PDE, a subject treated in greater detail in e.g. [70, 3]. To that end, let us denote the space of admissible shapes by $\mathcal{O}$ which consists of subsets of $\mathbb{R}^3$ satisfying some geometric a-priori regularity assumption that the design must conform. For each $\Omega \in \mathcal{O}$, let us assign function spaces $U(\Omega)$ and $V(\Omega)$ such a way that the *state equation*

$$A_\Omega u_\Omega = f_\Omega, \quad u_\Omega \in U(\Omega) \text{ and } f_\Omega \in V(\Omega), \tag{4.1}$$

describes the physics of the model given geometry Ω.

[1] See "Journal of Global Optimization", Springer.

For each $\Omega \in \mathcal{O}$ we attach a cost functional $\mathcal{J}_\Omega : U(\Omega) \to \mathbb{R}$. If the state equation has a unique solution u_Ω for each $\Omega \in \mathcal{O}$ we may consider the cost functional to be parametrized by Ω: $\hat{\mathcal{J}}(\Omega) = \mathcal{J}_\Omega(u_\Omega)$.

The abstract shape optimization problem is now given by:

$$\begin{aligned} &\text{Find } \Omega \in \mathcal{O} \text{ s.t.} \\ &\hat{\mathcal{J}}_\Omega(u_\Omega) \leq \hat{\mathcal{J}}_{\tilde{\Omega}}(u_{\tilde{\Omega}}), \quad \forall \tilde{\Omega} \in \mathcal{O}. \end{aligned} \tag{4.2}$$

In this thesis, the standpoint of Murat and Simon [75, 76] was taken implicitly and local variations of the reference domain Ω_0 as perturbations of identity are considered:

$$\Omega_\theta = \theta\Omega_0, \quad \|\theta - I\| < \epsilon, \tag{4.3}$$

where θ is in some Banach space of functions on $\mathbb{R}^3$ equipped with norm $\|\cdot\|$.

Suppose that there are pullbacks, i.e. operators arising from a function composition,

$$\begin{cases} \theta^* : U(\Omega_\theta) \longrightarrow U(\Omega_0) \\ \theta^* : V(\Omega_\theta) \longrightarrow V(\Omega_0) \end{cases} \tag{4.4}$$

induced by θ and that they are isomorphisms. Thus, we may consider a cost functional $\mathcal{J}$ depending explicitly on θ and $u \in U(\Omega_0)$ such a way that if $\theta^{-*}u_\theta$ (denoting $\theta^{-*} = (\theta^*)^{-1}$)) solves (4.1), then

$$\mathcal{J}(\theta, u_\theta) = \hat{\mathcal{J}}_{\Omega_\theta}(\theta^{-*}u_\theta). \tag{4.5}$$

Furthermore, we are in a position to pose the PDE restricted shape optimization problem as

$$\begin{aligned} &\underset{\substack{\|\theta\|<\epsilon \\ u_\theta \in U(\Omega)}}{\text{minimize}} \quad J(\theta, u_\theta) \\ &\text{subject to} \quad A_\theta u_\theta = f_\theta, \end{aligned} \tag{4.6}$$

where $A_\theta = \theta^* A_{\Omega_\theta} \circ \theta^{-*}$ and $f_\theta = \theta^* f_{\Omega_\theta}$.

Now we can differentiate $\mathcal{J}$ with respect to u and θ separately and use the chain rule:

$$\frac{d}{d\theta}\mathcal{J} = \frac{\partial \mathcal{J}}{\partial \theta} + \frac{\partial \mathcal{J}}{\partial u}\frac{\partial u}{\partial \theta}. \tag{4.7}$$

A particularly attractive approach to compute $\frac{d}{d\theta}\mathcal{J}(\theta, u_\theta)$ is the adjoint sensitivity method (see e.g. [77, 78, 70, 79, 80]). It can be derived from the constrained optimization problem with purely algebraic (and abstract) manipulations as follows.

Observing that the state equation $A_\theta u_\theta = f_\theta$ must hold for all θ, it holds that

$$0 = \frac{d}{d\theta}(A_\theta u_\theta - f_\theta) = \frac{\partial A}{\partial \theta}u + A\frac{\partial u}{\partial \theta} - \frac{\partial f}{\partial \theta} \tag{4.8}$$

and

$$\frac{\partial u}{\partial \theta} = A^{-1}\frac{\partial A}{\partial \theta}u - A^{-1}\frac{\partial f}{\partial \theta}. \tag{4.9}$$

Plugging this into (4.7) one obtains

$$\frac{d}{d\theta}\mathcal{J} = \frac{\partial \mathcal{J}}{\partial \theta} + \frac{\partial \mathcal{J}}{\partial u}A^{-1}\left(\frac{\partial A}{\partial \theta}u - \frac{\partial f}{\partial \theta}\right). \tag{4.10}$$

The operators $\frac{\partial \mathcal{J}}{\partial u}$ and A^{-1} do not depend on θ, and denoting $A'\gamma = \frac{\partial \mathcal{J}}{\partial u}'$, where A' is the adjoint of A, one finally obtains

$$\frac{d}{d\theta}\mathcal{J} = \frac{\partial \mathcal{J}}{\partial \theta} + \gamma'\left(\frac{\partial A}{\partial \theta}u - \frac{\partial f}{\partial \theta}\right). \tag{4.11}$$

Thus, the derivative $\frac{\partial A}{\partial \theta}$ needs to be evaluated.

In the next Section, the discrete EFIE system is fitted in to the framework above.

4.3 Application to discretized EFIE

Let us identify now Ω with the surface Γ, $U(\Gamma) = \mathbf{H}_{||}^{-\frac{1}{2}}(\nabla_\Gamma \cdot; \Gamma)$, $V(\Gamma) = \left(\mathbf{H}_{||}^{-\frac{1}{2}}(\nabla_\Gamma \cdot; \Gamma)\right)'$ and A_θ with the operator representation [33] of EFIE bilinear form.[2] Then, (4.6) can be written in the form

$$\begin{aligned} &\underset{\substack{\|\theta\|<\epsilon \\ \mathbf{j}\in\mathbf{H}_{||}^{-\frac{1}{2}}(\nabla_\Gamma\cdot;\Gamma)}}{\text{minimize}} \quad \mathcal{J}(\theta, \mathbf{j}) \\ &\text{subject to} \quad a(\theta^{-*}\mathbf{v}, \theta^{-*}\mathbf{j}; \Gamma_\theta) = \langle \theta^{-*\prime}\mathbf{E}^p, \mathbf{v}\rangle_\times, \quad \forall \mathbf{v} \in \mathbf{H}_{||}^{-\frac{1}{2}}(\nabla_\Gamma \cdot; \Gamma), \end{aligned} \tag{4.12}$$

where the bilinear form $a(\cdot, \cdot; \Gamma_\theta)$ is the one appearing in the RHS of EFIE (3.36)

$$\begin{aligned} a(\mathbf{u}, \mathbf{v}; \Gamma_\theta) = &- i\omega\mu \int_{\Gamma_\theta \times \Gamma_\theta} \mathbf{v}(\mathbf{r}) \cdot \mathbf{u}(\mathbf{r}')G(\mathbf{r} - \mathbf{r}')d\sigma_{\mathbf{r},\mathbf{r}'} - \\ &\frac{1}{i\omega\varepsilon}\int_{\Gamma_\theta \times \Gamma_\theta} \nabla_{\Gamma_\theta} \cdot \mathbf{v}(\mathbf{r})\nabla_{\Gamma_\theta} \cdot \mathbf{u}(\mathbf{r}')G(\mathbf{r} - \mathbf{r}')d\sigma_{\mathbf{r},\mathbf{r}'}, \end{aligned} \tag{4.13}$$

and $\theta^{-*\prime}$ is the adjoint of θ^{-*} with respect to the anti-linear pairing $\langle \cdot, \cdot \rangle_\times$.

In the Publication III the Piola transform discussed in section 3.2 was taken as the basis for the construction of the pullback θ^* for the EFIE discretized with the RT basis functions. The following change of variables formula was utilized to compute the $\frac{\partial A_\theta}{\partial \theta}$ type quantity:

[2] Recall that $'$ denotes duality.

If $\mathbf{v}, \mathbf{j} \in \mathcal{RT}(\Gamma)$, then it holds that

$$a(\mathcal{P}_\theta \mathbf{v}, \mathcal{P}_\theta \mathbf{j}; \Gamma_\theta) = \\ -\int_{\Gamma\times\Gamma} \left(i\omega\mu J_\theta \mathbf{v}(\mathbf{r}) \cdot J_\theta \mathbf{j}(\mathbf{r}') + \frac{1}{i\omega\varepsilon} \nabla_\Gamma \cdot \mathbf{v}(\mathbf{r}) \nabla_\Gamma \cdot \mathbf{j}(\mathbf{r}') \right) \\ G\left(\theta(\mathbf{r}) - \theta(\mathbf{r}')\right) d\sigma_{\mathbf{r},\mathbf{r}'}, \tag{4.14}$$

where J_θ is the Jacobian of θ.

The derivative of (4.14) has usually been evaluated with finite difference methods [77, 78] and recently with automatic differentiation [79, 80]. However, the finite difference and automatic differentiation do not compute the derivative of (4.14), instead it computes the derivative of numerical algorithm evaluating $a(\mathbf{v}, \mathbf{u}; \Gamma_\theta)$. From a more abstract point of view, the difference is obvious:

Let $f_s : x \mapsto f_s(x)$ be a function and let $\mathcal{A}_1^n$, $n = 1, 2, \cdots$, be a sequence of numerical algorithms such that

$$\mathcal{A}_1^n(f_s, x) \underset{n\to\infty}{\longrightarrow} f_s(x). \tag{4.15}$$

In exact arithmetic, applying finite difference formula to the above and taking limits results in

$$\lim_{s\to 0} \frac{1}{s} \left(\mathcal{A}_1^n(f_s, x) - \mathcal{A}_1^n(f_0, x) \right) = \frac{\partial}{\partial s} \mathcal{A}_1^n(f_s, x)\big|_{s=0}. \tag{4.16}$$

Now, even though $\mathcal{A}_1^n(f_s, x)$ might be a good approximation of $f_s(x)$, generally

$$\mathcal{A}_2^n\left(\frac{\partial f_s}{\partial s}\big|_{s=0}, x \right) \neq \frac{\partial}{\partial s} \mathcal{A}_1^n(f_s, x)\big|_{s=0}, \tag{4.17}$$

where $\mathcal{A}_2^n$ is another sequence of algorithms tailored to numerically evaluate the derivative:

$$\mathcal{A}_2^n\left(\frac{\partial f_s}{\partial s}\big|_{s=0}, x \right) \underset{n\to\infty}{\longrightarrow} \frac{\partial f_s(x)}{\partial s}\big|_{s=0}. \tag{4.18}$$

In Publication III an analytical integral formula for Gâteaux derivative of (4.14) was computed, and its numerical computation was addressed, when θ is such that it varies one vertex of the triangulation of Γ. It was pointed out that the expression of the differentiated system matrix contains the gradient of the Green's function, that can, and should, be transformed to an edge integral by integration by parts for reliable evaluation of the integral [81, 82]. Without such an analytical expression for the shape derivative integral at hand there is no formula to manipulate for a more reliable numerical evaluation.

5. First order system LL^* and extended Maxwell's equations

In this chapter discretization of the extended Maxwell's equations by the first order system LL^* method is discussed.

The FOSLL^* method is a rather young technique developed to treat non-smooth material parameters in the least squares finite element method [83, 5]. Furthermore, as we shall see in Section 5.2, such a formulation allows one to drop the requirement that RHS of the operator equation must be in L_2.

However, let us first illustrate (5.1) the low-frequency breakdown, usually plaguing the numerical methods derived from the reduced time-harmonic equations, with the curl curl equation.

5.1 Curl-curl equation and low-frequency breakdown

Let us consider the following popular ([29] and references therein) variational formulation for the reduced time-harmonic equations (2.16) with $\mathbf{n} \times \mathbf{E} = 0$ on $\partial\Omega$, $\mathbf{M} = 0$, Ω being simply connected and constant ε, μ:

$$\begin{aligned} &\text{Find } \mathbf{E} \in \mathbf{H}_0(\nabla\times, \Omega) \text{ s.t.} \\ &(\nabla \times \phi, \nabla \times \mathbf{E}) - \kappa^2(\phi, \mathbf{E}) = (\phi, \mathbf{F}), \quad \forall \phi \in \mathbf{H}_0(\nabla\times, \Omega), \end{aligned} \tag{5.1}$$

where $(\cdot, \cdot)$ is the L_2 inner product.

Let us denote $a_\kappa(\mathbf{u}, \mathbf{v}) = (\nabla \times \mathbf{u}, \nabla \times \mathbf{v}) - \kappa^2(\mathbf{u}, \mathbf{v})$ and the discrete lowest order Nédélec space [30] and its basis by

$$\operatorname{span}(\boldsymbol{\varphi}_n)_{n=1}^N = X_h \subset \mathbf{H}_0(\nabla\times, \Omega). \tag{5.2}$$

Furthermore, let us define a discrete norm on X_h by

$$|||\mathbf{u}_h|||^2 = \sum_n |\mathbf{u}_h^n|^2, \tag{5.3}$$

where $\mathbf{u}_h^n$ are the coefficients of $\mathbf{u}_h$ in the basis $(\boldsymbol{\varphi}_n)_n$.

The norms $\|\cdot\|_{L_2}$ and $|||\cdot|||$ are equivalent on X_h since X_h is a finite dimensional space. Thus, when considering the Rayleigh quotients

$$\frac{a_\kappa(\mathbf{u}_h, \mathbf{u}_h)}{|||\mathbf{u}_h|||^2}, \tag{5.4}$$

it suffices to inspect the ones given by the L_2-norm

$$\frac{a_\kappa(\mathbf{u}_h, \mathbf{u}_h)}{\|\mathbf{u}_h\|^2}. \tag{5.5}$$

When $\kappa \to 0$, the smallest Rayleigh quotient of a_κ tends to zero and, on the other hand, there are quotients that behave as $O(1)$:

If there is a constant $C > 0$ s.t.

$$C \geq \frac{|a_\kappa(\mathbf{u}, \mathbf{u})|}{\|\mathbf{u}\|^2} \tag{5.6}$$

for all $\mathbf{u} \in V_h$, then $C \leq |\kappa|^2$. This can be seen by taking $\mathbf{u} \in \nabla H^1 \cap X_h$. Note that the intersection is not empty because the gradients of first order nodal Lagrange functions whose support do not meet the edge of the computational domain are contained in X_h.

On the other hand, the space $\mathbf{H}_0(\nabla\times)$ supports a Helmholtz decomposition $\mathbf{H}_0(\nabla\times) = (\nabla H_0^1)^\perp \oplus \nabla H_0^1$ as subspaces of $\mathbf{L}_2$, where ∇H_0^1 is a closed subspace of $\mathbf{H}_0(\nabla\times)$ [29]. Thus, taking $\mathbf{u} \in X_h \cap (\nabla H_0^1)^\perp$ it holds that $\nabla \cdot \mathbf{u} = 0$ and using the Maxwell inequality (i.e. Friedrichs inequality [84, 85]) we get that there is a constant $c > 0$ not depending on $\mathbf{u}$ s.t.

$$\|\nabla \times \mathbf{u}\|^2 = \|\nabla \times \mathbf{u}\|^2 + \underbrace{\|\nabla \cdot \mathbf{u}\|^2}_{=0} \geq c\|\mathbf{u}\|_{L_2}^2. \tag{5.7}$$

Thus $|a_\kappa(\mathbf{u}, \mathbf{u})| \geq (c - \kappa^2)\|\mathbf{u}\|^2$.

This translates, in terms of the Rayleigh quotient of a_κ, to

$$c \leq \frac{|a_\kappa(\mathbf{u}, \mathbf{u})|}{\|\mathbf{u}\|^2}. \tag{5.8}$$

Thus the condition number of a_κ behaves as $O(|\kappa|^{-2})$ near zero wave number.

This phenomenon is called the *low-frequency breakdown*. In [86], Costabel introduces a penalty term $(\nabla \cdot \mathbf{u}, \nabla \cdot \mathbf{v})$ in the bilinear form, which eliminates the instability by making the bilinear form H^1-coercive. Another, purely numerical solution to the problem was proposed by Zhu et al in [11].

In this dissertation the low-frequency breakdown in finite element method is circumvented using the extended Maxwell's equations which then are discretized with a least squares finite element method [4]. More specifically,

the first order system LL^* [83, 5] is employed where the solution is sought as a minimizer of a certain problem dependent least-squares functional.

In the following, we review the FOSLL^* method and outline how the extended Maxwell's equations are discretized.

5.2 First order system LL^*

Let $\mathcal{H}$ be a Hilbert space and $L : \mathcal{D}(L) \subset \mathcal{H} \to \mathcal{H}$ an unbounded self-adjoint operator, with domain $\mathcal{D}(L)$. Consider the following equation in $\mathcal{H}$:

$$LU = F, \quad U \in \mathcal{D}(L). \tag{5.9}$$

Instead of solving this directly, one considers the least squares problem for the adjoint of L^* as

$$\min_{u \in \mathcal{D}(L^*)} \|L^*u - U\|^2_{\mathcal{H}}, \tag{5.10}$$

where U is the solution of (5.9).

Applying the variational argument to (5.10) results in an equivalent formulation:

$$\begin{aligned} &\text{Find } u \in \mathcal{D}(L^*) \text{ s.t.} \\ &(L^*u, L^*v) = (U, L^*v) \quad \forall v \in \mathcal{D}(L). \end{aligned} \tag{5.11}$$

It looks as if the original unknown U was needed to compute the right hand side of (5.11). However, because L^* is the adjoint of L, it holds that

$$(U, L^*v) = (LU, v) = (F, v). \tag{5.12}$$

In matrix computations this corresponds with the system

$$\mathbf{A}\mathbf{A}^H\mathbf{y} = \mathbf{b}. \tag{5.13}$$

If the sesquilinear form (L^*u, L^*v) is elliptic and bounded, the problem (5.11) has a unique solution by Lax-Milgram theorem. However, because L and L^* are a-priori unbounded operators, the boundedness needs to be considered in new a energy norm on $\mathcal{D}(L)$.

To that end, let us turn to the extended Maxwell's equations for normalized fields and state their properties discussed in greater detail in [13, 84].

Let $\mathcal{H} = (L_2)^8$ and

$$L = \mathcal{P} - i\kappa I,$$

where I is the identity operator, $\kappa = \omega\sqrt{\varepsilon\mu}$ and

$$\mathcal{P} = \begin{bmatrix} 0 & 0 & \nabla\cdot & 0 \\ 0 & 0 & -\nabla\times & \nabla \\ \nabla & \nabla\times & 0 & 0 \\ 0 & \nabla\cdot & 0 & 0 \end{bmatrix}. \tag{5.14}$$

For extended Maxwell's equations the F on the RHS of the Equation (5.9) consists of charge and current densities:

$$F = \begin{bmatrix} 0 & \sqrt{\mu}\mathbf{J} & 0 & \frac{\rho}{\sqrt{\varepsilon}} \end{bmatrix}^{\mathsf{T}} \tag{5.15}$$

Packing the fields in to the variable U as

$$U = \begin{bmatrix} \Phi & \mathbf{E} & \mathbf{H} & \Psi \end{bmatrix}^{\mathsf{T}}, \tag{5.16}$$

where Φ and Ψ are slack variables needed to square Maxwell's equations and $\mathbf{E}$ and $\mathbf{H}$ are the normalized fields (2.17), we find that the operator equation

$$LU = F \tag{5.17}$$

is just a rewording of the extended Maxwell's equations.

If $\mathcal{D}(L)$ is given by

$$\mathcal{D}_E(\Omega) = H^1\big(\Omega\big)/\mathbb{C} \times \mathbf{H}_{\underset{DC}{\circ}}(\Omega) \times \mathbf{H}_{\underset{DC}{\circ}}(\Omega) \times H_0^1(\Omega) \quad \text{or} \tag{5.18}$$

$$\mathcal{D}_M(\Omega) = H_0^1(\Omega) \times \mathbf{H}_{\underset{DC}{\circ}}(\Omega) \times \mathbf{H}_{\underset{DC}{\circ}}(\Omega) \times H^1(\Omega)\big/\mathbb{C}, \tag{5.19}$$

where

$$\begin{cases} \mathbf{H}_{\underset{DC}{\circ}} = \mathbf{H}_0(\nabla\cdot) \cap \mathbf{H}(\nabla\times) \quad \text{and} \\ \mathbf{H}_{\underset{DC}{\circ}} = \mathbf{H}(\nabla\cdot) \cap \mathbf{H}_0(\nabla\times), \end{cases}$$

then it holds that $\mathcal{D}(L) = \mathcal{D}(L^*)$ and, furthermore, $L^* = -L$ if $\kappa \in \mathbb{R}$.

Considering $\mathcal{D}_R$ ($R = E, M$) as a Sobolev space equipped with a norm given by

$$\begin{aligned} \Big\|\begin{bmatrix} \Phi & \mathbf{E} & \mathbf{H} & \Psi \end{bmatrix}\Big\|_{\mathcal{D}} = \Big(\Big\|\begin{bmatrix} \Phi & \mathbf{E} & \mathbf{H} & \Psi \end{bmatrix}\Big\|_{\mathcal{H}} \\ + \|\nabla\cdot\mathbf{H}\|_{L_2}^2 + \|\nabla\cdot\mathbf{E}\|_{L_2}^2 \\ + \|\nabla\times\mathbf{H}\|_{L_2}^2 + \|\nabla\times\mathbf{E}\|_{L_2}^2 \\ + \|\nabla\Psi\|_{L_2}^2 + \|\nabla\Phi\|_{L_2}^2 \Big)^{\frac{1}{2}} \end{aligned} \tag{5.20}$$

it holds that there are constants $C, c > 0$ not depending on $u \in \mathcal{D}_R$ s.t.

$$c\|u\|_{\mathcal{D}} \leq \|Lu\| \leq C\|U\|_{\mathcal{D}}. \tag{5.21}$$

Thus, the bilinear form (L^*u, L^*v) $\mathcal{D}_R$-elliptic.

The abstract least squares variational formulation (5.11) takes the following form:

$$\begin{aligned} &\text{Find } u \in \mathcal{D}_R \text{ s.t.} \\ &((\mathcal{P}^* + i\overline{\kappa}I)u, (\mathcal{P}^* + i\overline{\kappa}I)v) = (U, (\mathcal{P}^* + i\overline{\kappa}I)v), \quad \forall v \in \mathcal{D}_R. \end{aligned} \tag{5.22}$$

Defining matrix $P(\mathbf{n})$ by

$$P(\mathbf{n}) = \begin{bmatrix} 0 & 0 & \mathbf{n}\cdot & 0 \\ 0 & 0 & -\mathbf{n}\times & \mathbf{n} \\ \mathbf{n} & \mathbf{n}\times & 0 & 0 \\ 0 & \mathbf{n}\cdot & 0 & 0 \end{bmatrix}, \tag{5.23}$$

the following formal integration by parts formula holds

$$(\mathcal{P}U, V) + (U, \mathcal{P}V) = \int_{\partial\Omega} P(\mathbf{n})U \cdot \overline{V} d\sigma. \tag{5.24}$$

Thus, the right hand side of (5.22) is given by

$$\begin{aligned} (U, L^*v) &= \int_{\partial\Omega} P(\mathbf{n})U \cdot \overline{v} d\sigma + (LU, v) \\ &= \int_{\partial\Omega} P(\mathbf{n})U \cdot \overline{v} d\sigma + (F, v) \end{aligned} \tag{5.25}$$

Moreover, if $v \in \mathcal{D}_R(\Omega)$ then, denoting $v = \begin{bmatrix} f & \boldsymbol{\varepsilon} & \boldsymbol{\chi} & p \end{bmatrix}^\intercal$, the surface integral above results in

$$\int_{\partial\Omega} P(\mathbf{n}) \cdot \overline{v} d\sigma = \begin{cases} \displaystyle\int_{\partial\Omega} \overline{f}\mathbf{n} \cdot \mathbf{H} + \Psi\mathbf{n} \cdot \overline{\boldsymbol{\varepsilon}} + \overline{\boldsymbol{\chi}} \cdot \mathbf{n} \times \mathbf{E} d\sigma & v \in \mathcal{D}_E, \\ \displaystyle\int_{\partial\Omega} \Phi\mathbf{n} \cdot \overline{\boldsymbol{\chi}} + \overline{p}\mathbf{n} \cdot \mathbf{E} - \overline{\boldsymbol{\varepsilon}} \cdot \mathbf{n} \times \mathbf{H} d\sigma & v \in \mathcal{D}_M. \end{cases} \tag{5.26}$$

Supposing that there is a family approximating discrete subspaces $\boldsymbol{X}_R^h$ of $\mathcal{D}_R$, then the discrete form of (5.22) is

$$\begin{aligned} &\text{Find } u \in \boldsymbol{X}_R^h \text{ s.t.} \\ &(L^*u, L^*v) = (F, v) + \int_{\partial\Omega} P(\mathbf{n})U \cdot v d\sigma, \quad \forall v \in \boldsymbol{X}_R^h. \end{aligned} \tag{5.27}$$

If u is the solution of the problem (5.22), then the original electromagnetic field U is given by $U = (\mathcal{P}^* + i\overline{\kappa})u$. Thus, u could be called *dual-potential* of U. Indeed, denoting $u = \begin{bmatrix} \varphi & \mathbf{e} & \mathbf{h} & \psi \end{bmatrix}$ and $v = \begin{bmatrix} f & \boldsymbol{\varepsilon} & \boldsymbol{\chi} & p \end{bmatrix}$, when $\kappa = 0$ the bilinear form in (5.22) reduces to

$$\begin{aligned} &(\nabla \cdot \mathbf{h}, \nabla \cdot \boldsymbol{\chi}) + (\nabla \times \mathbf{h}, \nabla \times \boldsymbol{\chi}) + (\nabla\psi, \nabla p) + \\ &(\nabla \cdot \mathbf{e}, \nabla \cdot \boldsymbol{\varepsilon}) + (\nabla \times \mathbf{e}, \nabla \times \boldsymbol{\varepsilon}) + (\nabla\varphi, \nabla f) = (-\mathbf{J}, \boldsymbol{\varepsilon}) + (\rho, p). \end{aligned} \tag{5.28}$$

Thus, $\mathbf{e}$ is the vector potential of $\mathbf{H}$ and ψ is the scalar potential of $\mathbf{E}$ arising from impressed the current $\mathbf{J}$ and charge ρ.

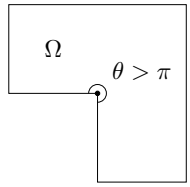

Figure 5.1. A domain Ω with a re-entrant corner in which Gaffney's inequality does not hold.

It should be noted that even though the solution to the original operator equation was sought from $\mathcal{D}_R$, the minimization of the least squares functional for the adjoint operator allows the solution U to be in L_2: The Lax-Milgram lemma guarantees that the variational problem (5.11) has a unique solution if $v \mapsto (v, L^*U)$ is a continuous linear functional on $\mathcal{D}_R$.

The drawback, or virtue, of the present approach is that one is required to use H^1 conforming discretization owing to the presence of the div-curl Sobolev spaces $\mathbf{H}_{\overset{\circ}{DC}}$ and $\mathbf{H}_{D\overset{\circ}{C}}$. Although such a discretization is easy to implement at relatively high orders, the downside is that the computational domain must exhibit enough regularity for the Gaffney's (or Friedrich's) inequality [87, 88]

$$c\|\mathbf{u}\|_{H^1} \leq \|\mathbf{u}\| + \|\nabla \cdot \mathbf{u}\| + \|\nabla \times \mathbf{u}\| \tag{5.29}$$

to hold.

The inequality holds if Ω is smooth or convex, but if it has a re-entrant corner, such as depicted in Fig. 5.1, $\mathbf{H}_{\overset{\circ}{DC}}(\Omega) \cap (H^1(\Omega))^n$, $n \in \{2, 3\}$, is a closed proper subspace of $\mathbf{H}_{\overset{\circ}{DC}}(\Omega)$ [86, 24], i.e. there can be no continuous embedding $\mathbf{H}_{\overset{\circ}{DC}}(\Omega) \hookrightarrow (H^1(\Omega))^n$. In such domains there are functions that belong to $\mathbf{H}_{\overset{\circ}{DC}}(\Omega)$, that cannot be approximated with $(H^1(\Omega))^n$ functions in $(H^1(\Omega))^n$ norm, the standard a priori approximation results (see [33]) of H^1 elements are not available and, moreover, it has been observed numerically that the convergence deteriorates [89].

Another challenge in H^1 conforming finite element bases is that in some cases vanishing normal (or tangential) component implies vanishing tangential component also. Thus, boundary conditions such as $\mathbf{n} \cdot \mathbf{F} = 0$ need to be relaxed. For example, in a polyhedral domain approximating a circular disc, if a first order Lagrange nodal vectorial basis function has zero normal trace, then it vanishes on the boundary. Instead, if the normal trace for $\boldsymbol{\psi} \in (S_{h,1})^2$ is imposed in a weak sense by requiring that

$$\int_\Omega \nabla \cdot \boldsymbol{\psi}\phi - \boldsymbol{\psi} \cdot \nabla\phi dx = 0 \quad \forall \phi \in S_{h,1} \tag{5.30}$$

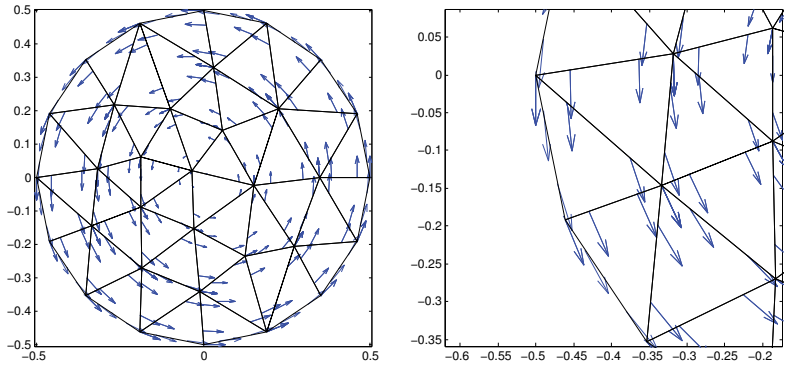

Figure 5.2. A non-conformal vector field satisfying vanishing discrete weak normal trace (left). A closeup on the field near boundary (right).

holds, one ends up with a non-conformal discretization that can represent functions such as shown in Figure 5.2.

6. Summary of the publications

Publication I The Publication I was devoted to construction of a good parametrization for the shapes of planar wire dipoles and its demonstration in directivity and input impedance optimization. The work is continuation of the author's M.Sc. thesis in which the Landstorfer's shaped dipole antenna [69] was re-optimized with modern full-wave methods.

The parametrization was based on interpreting a point on S^1 as a tangent vector of a curve and integrating the vector resulting in an arc-length parametrized curve. The regularity of the curve was deducted from physical properties that bent metallic wires must possess: no self-intersections, finite length and lower bound for the radius of curvature.

Publication II In the second publication the shape derivatives of the discrete MFIE system were derived and evaluated against finite difference formula. It also provides a non-trivial example where existing singularity subtraction technique cannot be used. Instead, fully numerical high precision singularity cancellation rules [90] were used.

Publication III In this publication, the shape derivative formulas for the system matrix of the EFIE were derived for the first time and they were compared against automatic differentiation method and finite differences.

It was shown that if the shape derivative integrals are integrated in a particular manner , the relative difference with AD and FD methods are optimal, i.e., up to floating point precision for AD and half of the floating point precision for FD. However, because the resulting differentiated integrals are more singular they should be integrated using techniques described in [91, 81]. Utilizing those integration methods described in the relative difference of a system matrix arising from a real world example turns out to be of order 10^{-3} instead of the expected 10^{-8}.

Work closest to the Publication III is the paper by Ureel and De Zutter [92] where they solved the problem of finding shape derivative of surface

current in case of planar microstrip structures with mixed potential integral equation (see e.g. [93, 94]). Their approach is based on Reynolds parallel transport theorem, i.e. differentiation under the integral sign, and it is limited to planar perturbations of the edges of the metallization.

Other important pieces of work include Potthast's paper [95] where the Fréchet differentiability of the scattered field from a PEC obstacle with respect to small variations of the boundary is addressed in the framework of Hölder spaces. Furthermore, the first derivative of the scattered field is characterised as a solution of a new boundary value problem. In papers [96, 97] Le Louër and Costabel extend Potthast's work to dielectric transmission problem in Sobolev spaces. These pieces of work are, however, rather theoretical from the point of view of computational electromagnetics and, more importantly, they do not address the adjoint variable method.

Publication IV In the Publication IV techniques discussed in the Publications II and III were utilized in a sensitivity analysis and optimization of electrically large structures. The shape sensitivity computation was based on calculation of the derivatives of the MLFMA process and was implemented by rewriting parts of an existing MLFMA code. In this publication also two validating optimization examples were presented.

Publication V In this publication the FOSLL^* method applied to electromagnetics was examined in three dimensional domains. In it the effect of interior resonances of the domain was presented and it was shown how the formulation can be used as a hybrid method. The weakly tangential or normal discrete FE spaces were implemented using orthogonal projections that take the finite element functions to the right subspaces. More specifically, at each Krylov iteration the new generated vector was projected to the FE subspace satisfying the discrete weak boundary condition and the projections were generated using the SVD. It was also shown that the discrete variational form is elliptic in the space where discrete weak boundary conditions hold when the mesh is fine enough.

References

[1] J. C. Maxwell, "A dynamical theory of the electromagnetic field," *Philosophical Transactions of the Royal Society of London*, vol. 155, pp. 459–512, 1865.

[2] J. Maxwell, *A Treatise on Electricity and Magnetism*. Oxford: Clarendon press, 1873.

[3] J. Sokołowski and J. Zolésio, *Introduction to Shape Optimization: Shape Sensitivity Analysis*. Springer series in computational mathematics, Springer-Verlag, 1992.

[4] P. Bochev and M. Gunzburger, *Least-Squares Finite Element Methods*. Applied Mathematical Sciences, Springer, 2009.

[5] A. M. Thomas, F. M. Stephen, R. John, and J. Schmidt, "First-order system LL* (FOSLL*) for general scalar elliptic problems in the plane," *SIAM J. Numerical Analysis*, vol. 43, no. 5, pp. 2098–2120, 2005.

[6] R. Picard, "On a structural observation in generalized electromagnetic theory," *Journal of Mathematical Analysis and Applications*, vol. 110, no. 1, pp. 247–264, 1985.

[7] J. D. Jackson, *Classical Electrodynamics*. Wiley, third ed., 1998.

[8] F. Hehl and I. Obukhov, *Foundations of Classical Electrodynamics: Charge, Flux, and Metric*, vol. 33. Springer, 2003.

[9] J. Z. Zhao and C. Weng, "Integral equation solution of Maxwell's equations from zero frequency to microwave frequencies," *IEEE Transactions on Antennas and Propagation*, vol. 48, no. 10, pp. 1635–1645, 2000.

[10] M. Taskinen and P. Yla-Oijala, "Current and charge integral equation formulation," *IEEE Transactions on Antennas and Propagation*, vol. 54, pp. 58 – 67, jan. 2006.

[11] J. Zhu and D. Jiao, "A rigorous solution to the low-frequency breakdown in full-wave finite-element-based analysis of general problems involving inhomogeneous lossless/lossy dielectrics and nonideal conductors," *IEEE Transactions on Microwave Theory and Techniques*, vol. 59, no. 12, pp. 3294–3306, 2011.

[12] R. Picard, "On the low frequency asymptotics in electromagnetic theory," *Journal für die reine und angewandte Mathematik*, vol. 1984, pp. 50–73, 1984.

[13] R. Leis, *Initial Boundary Value Problems in Mathematical Physics*. Teubner, 1986.

[14] P. Ola and E. Somersalo, "Electromagnetic inverse problems and generalized sommerfeld potentials," *SIAM Journal on Applied Mathematics*, vol. 56, no. 4, pp. 1129–1145, 1996.

[15] R. Picard, "On the boundary value problems of electro- and magnetostatics," *Proceedings of the Royal Society of Edinburgh: Section A Mathematics*, vol. 92, pp. 165–174, 1 1982.

[16] J. Stratton, *Electromagnetic Theory*. International series in pure and applied physics, McGraw-Hill book company, inc., 1941.

[17] J. Nedelec, *Acoustic and Electromagnetic Equations: Integral Representations for Harmonic Problems*. Springer, 2001.

[18] R. F. Harrington, *Field Computation by Moment Methods*. Wiley-IEEE Press, 1993.

[19] P. Grisvard, *Elliptic Problems in Nonsmooth Domains*. Pitman (Advanced Publishing Program), 1985.

[20] S. Hofmann, M. Mitrea, and M. Taylor, "Geometric and transformational properties of Lipschitz domains, Semmes-Kenig-Toro domains, and other classes of finite perimeter domains," *The Journal of Geometric Analysis*, vol. 17, no. 4, pp. 593–647, 2007.

[21] L. C. Evans and R. F. Gariepy, *Measure Theory and Fine Properties of Functions*. CRC Press, 1992.

[22] W. Rudin, *Functional analysis*. International Series in Pure and Applied Mathematics, New York: McGraw-Hill Inc., second ed., 1991.

[23] E. Gagliardo, "Caratterizzazioni delle tracce sulla frontiera relative ad alcune classi di funzioni in n variabili," *Rendiconti del seminario matematico della università di Padova*, vol. 27, pp. 284–305, 1957.

[24] V. Girault and P. Raviart, *Finite Element Methods for Navier-Stokes Equations: Theory and Algorithms*. Springer-Verlag, 1986.

[25] L. Tartar, "On the characterization of traces of a Sobolev space used for Maxwell's equation," in *Proceedings of a Meeting Held in Bordeaux, in Honour of Michel Artola* (A.-Y. L. Roux, ed.), November 1997.

[26] A. Buffa and P. Ciarlet, "On traces for functional spaces related to Maxwell's equations part I: An integration by parts formula in Lipschitz polyhedra," *Mathematical Methods in the Applied Sciences*, vol. 24, no. 1, pp. 9–30, 2001.

[27] A. Buffa, M. Costabel, and D. Sheen, "On traces for $H(curl, \Omega)$ in Lipschitz domains," *Journal of Mathematical Analysis and Applications*, vol. 276, no. 2, pp. 845 – 867, 2002.

[28] P. G. Ciarlet, *The Finite Element Method for Elliptic Problems*. North-Holland, 1978.

[29] P. Monk, *Finite Element Methods for Maxwell's Equations*. Numerical Analysis and Scientific Computation Series, Clarendon Press, 2003.

[30] J. Nedelec, "Mixed finite elements in $\mathbb{R}^3$," *Numerische Mathematik*, vol. 35, no. 3, pp. 315–341, 1980.

[31] P.-A. Raviart and J. M. Thomas, "A mixed finite element method for 2nd order elliptic problems," in *Mathematical Aspects of Finite Element Methods (Proc. Conf., Consiglio Naz. delle Ricerche (C.N.R.), Rome, 1975)*, pp. 292–315. Lecture Notes in Math., vol. 606, Berlin: Springer, 1977.

[32] S. Rao and A. Wilton D.R.and Glisson, "Electromagnetic scattering by surfaces of arbitrary shape," *IEEE Transactions on Antennas and Propagation*, vol. 30, pp. 409–418, May 1982.

[33] D. Braess, *Finite Elements: Theory, Fast Solvers, and Applications in Solid Mechanics*. Cambridge University Press, 2001.

[34] A. Logg, K.-A. Mardal, G. N. Wells, *et al.*, *Automated Solution of Differential Equations by the Finite Element Method*. Springer, 2012.

[35] J. A. Stratton and L. J. Chu, "Diffraction theory of electromagnetic waves," *Physical Review*, vol. 56, pp. 99–107, July 1939.

[36] V. H. Rumsey, "Reaction concept in electromagnetic theory," *Phys. Rev.*, vol. 94, pp. 1483–1491, June 1954.

[37] D. Mitrea, M. Mitrea, and J. Pipher, "Vector potential theory on nonsmooth domains in R^3 and applications to electromagnetic scattering," *Journal of Fourier Analysis and Applications*, vol. 3, no. 2, pp. 131–192, 1996.

[38] G. Verchota, "Layer potentials and regularity for the Dirichlet problem for Laplace's equation in Lipschitz domains," *Journal of Functional Analysis*, vol. 59, no. 3, pp. 572 – 611, 1984.

[39] J. R. Mautz and R. F. Harrington, "H-field, E-field, and combined field solutions for bodies of revolution," tech. rep., DTIC Document, 1977.

[40] R. F. Harrington, "Boundary integral formulations for homogeneous material bodies," *Journal of Electromagnetic Waves and Applications*, vol. 3, pp. 1–15, 1989.

[41] P. Ylä-Oijala, M. Taskinen, and S. Järvenpää, "Analysis of surface integral equations in electromagnetic scattering and radiation problems," *Engineering Analysis with Boundary Elements*, vol. 32, no. 3, pp. 196–209, 2008.

[42] O. Ergul and L. Gurel, "Efficient parallelization of the multilevel fast multipole algorithm for the solution of large-scale scattering problems," *IEEE Transactions on Antennas and Propagation*, vol. 56, no. 8, pp. 2335–2345, 2008.

[43] O. Ergul and L. Gurel, "Parallel-MLFMA solution of CFIE discretized with tens of millions of unknowns," in *The Second European Conference on Antennas and Propagation, EuCAP 2007*, pp. 1–7, 2007.

[44] K. Cools, F. Andriulli, D. De Zutter, and E. Michielssen, "Accurate and conforming mixed discretization of the mfie," *IEEE Antennas and Wireless Propagation Letters*, vol. 10, pp. 528–531, 2011.

[45] A. Buffa and S. Christiansen, "A dual finite element complex on the barycentric refinement," *Mathematics of Computation*, vol. 76, no. 260, pp. 1743–1769, 2007.

[46] F. Andriulli, K. Cools, H. Bagci, F. Olyslager, A. Buffa, S. Christiansen, and E. Michielssen, "A multiplicative calderon preconditioner for the electric field integral equation," *IEEE Transactions on Antennas and Propagation*, vol. 56, pp. 2398–2412, Aug 2008.

[47] P. Yla-Oijala, S. Kiminki, and S. Jarvenpaa, "Solving IBC-CFIE with dual basis functions," *IEEE Transactions on Antennas and Propagation*, vol. 58, pp. 3997–4004, Dec 2010.

[48] H. Bağci, F. Andriulli, K. Cools, F. Olyslager, and E. Michielssen, "A Calderón multiplicative preconditioner for the combined field integral equation," *IEEE Transactions on Antennas and Propagation*, vol. 57, pp. 3387–3392, Oct 2009.

[49] A. Buffa and P. Ciarlet, "On traces for functional spaces related to Maxwell's equations part II: Hodge decompositions on the boundary of Lipschitz polyhedra and applications," *Mathematical Methods in the Applied Sciences*, vol. 24, no. 1, pp. 31–48, 2001.

[50] R. Hiptmair and C. Schwab, "Natural boundary element methods for the electric field integral equation on polyhedra," *SIAM Journal on Numerical Analysis*, vol. 40, no. 1, pp. 66–86, 2002.

[51] V. Rokhlin, "Diagonal forms of translation operators for the Helmholtz equation in three dimensions," *Applied and Computational Harmonic Analysis*, vol. 1, no. 1, pp. 82 – 93, 1993.

[52] R. Coifman, V. Rokhlin, and S. Wandzura, "The fast multipole method for the wave equation: A pedestrian prescription," *IEEE Antennas Propag. Mag.*, vol. 35, no. 3, pp. 7–12, 1993.

[53] W. Chew, J.-M. Jin, E. Michielssen, and J. Song, *Fast and Efficient Algorithms in Computational Electromagnetics*. Antennas and Propagation Library, Artech House, Incorporated, 2001.

[54] S. Järvenpää and P. Ylä-Oijala, "A global interpolator with low sample rate for multilevel fast multipole algorithm," *IEEE Transactions on Antennas and Propagation*, vol. 61, no. 3, pp. 1291–1300, 2013.

[55] C. Cecka and E. Darve, "Fourier-based fast multipole method for the helmholtz equation," *SIAM J. Sci. Comput.*, vol. 35, no. 1, pp. A79–A103, 2013.

[56] M. Abramowitz and I. A. Stegun, *Handbook of Mathematical Functions, With Formulas, Graphs, and Mathematical Tables*. New York: Dover, 1964.

[57] Q. Carayol and F. Collino, "Error estimates in the fast multipole method for scattering problems part 2: Truncation of the gegenbauer series," *ESAIM: Mathematical Modelling and Numerical Analysis*, vol. 39, pp. 183–221, 1 2005.

[58] T. Dufva and J. Sarvas, "Broadband MLFMA with plane wave expansions and optimal memory demand," *IEEE Transactions on Antennas and Propagation*, vol. 57, pp. 742–753, March 2009.

[59] S. Jarvenpaa and P. Yla-Oijala, "Multilevel fast multipole algorithm with global and local interpolators," *IEEE Transactions on Antennas and Propagation*, vol. 62, pp. 4716–4725, Sept 2014.

[60] H. Yagi and S. Uda, "Projector of the sharpest beam of electric waves," *Proceedings of the Imperial Academy (of Japan)*, vol. 2, pp. 49–52, February 1926.

[61] D. Cheng, "Gain optimization for Yagi-Uda arrays," *IEEE Antennas and Propagation Magazine*, vol. 33, no. 3, pp. 42–46, 1991.

[62] C. Chen and D. Cheng, "Optimum element lengths for Yagi-Uda arrays," *IEEE Transactions on Antennas and Propagation*, vol. 23, no. 1, pp. 8–15, 1975.

[63] J. Bojsen, H. Schjaer-Jacobsen, E. Nilsson, and J. Bach Andersen, "Maximum gain of Yagi-Uda arrays," *Electronics Letters*, vol. 7, no. 18, pp. 531–532, 1971.

[64] L. C.-H and D. Cheng, "Directivity optimization for Yagi-Uda arrays of shaped dipoles," *IEEE Transactions on Antennas and Propagation*, vol. 31, no. 3, pp. 522–525, 1983.

[65] N. Kaneda, W. Deal, Y. Qian, R. Waterhouse, and T. Itoh, "A broadband planar quasi-yagi antenna," *IEEE Transactions on Antennas and Propagation*, vol. 50, no. 8, pp. 1158–1160, 2002.

[66] H. Ehrenspeck and H. Poehler, "A new method for obtaining maximum gain from Yagi antennas," *IRE Transactions on Antennas and Propagation*, vol. 7, no. 4, pp. 379–386, 1959.

[67] J. Nocedal and S. Wright, *Numerical Optimization*. Springer, 1999.

[68] Y. T. Lo, "A note on the cylindrical antenna of noncircular cross section," *J. Appl. Phys*, vol. 24, pp. 1338–1339, Oct 1953.

[69] F. Landstorfer, "Zur optimalen form von linearantennen," *Frequenz*, vol. 30, no. 12, pp. 344–349, 1976.

[70] J. Haslinger and R. Mäkinen, *Introduction to Shape Optimization: Theory, Approximation, and Computation*. Advances in Design and Control, Society for Industrial and Applied Mathematics, 2003.

[71] E. Jones and W. Joines, "Design of Yagi-Uda antennas using genetic algorithms," *IEEE Transactions on Antennas and Propagation*, vol. 45, pp. 1386–1392, Sep 1997.

[72] M. Cismasu and M. Gustafsson, "Illustration of mobile terminal antenna optimization by genetic algorithms with single frequency simulation," in *Proceedings of 2013 URSI International Symposium on Electromagnetic Theory (EMTS)*, pp. 84–87, May 2013.

[73] U. Singh, M. Rattan, N. Singh, and M. Patterh, "Design of a yagi-uda antenna by simulated annealing for gain, impedance and fbr," in *IET-UK International Conference on Information and Communication Technology in Electrical Sciences (ICTES 2007)*, pp. 974–979, Dec 2007.

[74] R. L. Haupt and D. H. Werner, *Genetic Algorithms in Electromagnetics*. Wiley-IEEE Press, 2007.

[75] J. Simon, "Differentiation with respect to the domain in boundary value problems," *Numerical Functional Analysis and Optimization*, vol. 2, no. 7-8, pp. 649–687, 1980.

[76] F. Murat and J. Simon, "Etude de problème d'optimal design," in *Optimization Techniques*, pp. 54–62, 1975.

[77] N. Nikolova, J. Bandler, and M. Bakr, "Adjoint techniques for sensitivity analysis in high-frequency structure CAD," *IEEE Transactions on Microwave Theory and Techniques*, vol. 52, pp. 403 – 419, Jan. 2004.

[78] N. Nikolova, J. Zhu, D. Li, M. Bakr, and J. Bandler, "Sensitivity analysis of network parameters with electromagnetic frequency-domain simulators," *IEEE Transactions on Microwave Theory and Techniques*, vol. 54, no. 2, pp. 670 – 681, 2006.

[79] J. I. Toivanen, R. A. E. Mäkinen, S. Järvenpää, P. Ylä-Oijala, and J. Rahola, "Electromagnetic sensitivity analysis and shape optimization using method of moments and automatic differentiation," *IEEE Transactions on Antennas Propagation*, vol. 57, no. 1, pp. 168–175, 2009.

[80] J. Toivanen, R. E. Mäkinen, J. Rahola, S. Järvenpää, and P. Ylä-Oijala, "Gradient-based shape optimisation of ultra-wideband antennas parameterised using splines," *IET Microwaves, Antennas and Propagation*, vol. 4, pp. 1406–1414, 2010.

[81] S. Järvenpää, M. Taskinen, and P. Ylä-Oijala, "Singularity subtraction technique for high-order polynomial vector basis functions on planar triangles," *IEEE Transactions on Antennas and Propagation*, vol. 54, pp. 42 – 49, Jan. 2006.

[82] I. Hänninen, M. Taskinen, and J. Sarvas, "Singularity subtraction integral formulae for surface integral equations with RWG, rooftop and hybrid basis functions," *IEEE Transactions on Antennas and Propagation*, vol. 53, October 2005.

[83] Z. Cai, T. Manteuffel, S. McCormick, and J. Ruge, "First-order system LL^* (FOSLL*): Scalar elliptic partial differential equations," *SIAM J. Numerical Analysis*, vol. 39, no. 4, pp. 1418–1445, 2001.

[84] P. Neff, D. Pauly, and K.-J. Witsch, "Maxwell meets Korn: A new coercive inequality for tensor fields in $\mathbb{R}^{N\times N}$ with square-integrable exterior derivative," *Mathematical Methods in the Applied Sciences*, vol. 35, no. 1, pp. 65–71, 2012.

[85] R. Picard, "An elementary proof for a compact imbedding result in generalized electromagnetic theory," *Mathematische Zeitschrift*, vol. 187, pp. 151–164, 1984.

[86] M. Costabel, "A coercive bilinear form for Maxwell's equations," *Journal of Mathematical Analysis and Applications*, vol. 157, no. 2, pp. 527 – 541, 1991.

[87] M. P. Gaffney, “Hilbert space methods in the theory of harmonic integrals,” *Transactions of the American Mathematical Society*, vol. 78, no. 2, pp. 426–444, 1955.

[88] K. O. Friedrichs, “Differential forms on Riemannian manifolds,” *Communications on Pure and Applied Mathematics*, vol. 8, no. 4, pp. 551–590, 1955.

[89] E. Lee and T. A. Manteuffel, “FOSLL* method for the eddy current problem with three-dimensional edge singularities,” *SIAM J. Numerial Analysis*, vol. 45, no. 2, pp. 787–809, 2007.

[90] A. Polimeridis, F. Vipiana, J. Mosig, and D. Wilton, “DIRECTFN: Fully numerical algorithms for high precision computation of singular integrals in Galerkin SIE methods,” *IEEE Transactions on Antennas and Propagation*, 2013.

[91] P. Ylä-Oijala and M. Taskinen, “Calculation of CFIE impedance matrix elements with RWG and n x RWG functions,” *IEEE Transactions on Antennas and Propagation*, vol. 51, no. 8, pp. 1837–1846, 2003.

[92] J. Ureel and D. De Zutter, “A new method for obtaining the shape sensitivities of planar microstrip structures by a full-wave analysis,” *IEEE Transactions on Microwave Theory and Techniques*, vol. 44, no. 2, pp. 249–260, 1996.

[93] K. A. Michalski, “The mixed-potential electric field integral equation for objects in layered media,” *Archiv Elektronik und Uebertragungstechnik*, vol. 39, pp. 317–322, 1985.

[94] J. Mosig, “Arbitrarily shaped microstrip structures and their analysis with a mixed potential integral equation,” *IEEE Transactions on Microwave Theory and Techniques*, vol. 36, no. 2, pp. 314–323, 1988.

[95] R. Potthast, “Domain derivatives in electromagnetic scattering,” *Mathematical Methods in the Applied Sciences*, vol. 19, no. 15, pp. 1157–1175, 1996.

[96] M. Costabel and L. L. F., “Shape derivatives of boundary integral operators in electromagnetic scattering,” *arXiv*, 2010, arXiv:1002.1541v2 [math.NA].

[97] M. Costabel and F. Le Louër, “Shape derivatives of boundary integral operators in electromagnetic scattering. part II: Application to scattering by a homogeneous dielectric obstacle,” *arXiv*, 2011, arXiv:1105.2479v1 [math.NA].

Aalto-DD 155/2014

ISBN 978-952-60-5898-6
ISBN 978-952-60-5899-3 (pdf)
ISSN-L 1799-4934
ISSN 1799-4934
ISSN 1799-4942 (pdf)

Aalto University
School of Electrical Engineering
Department of Radio Science and Engineering
www.aalto.fi

BUSINESS +
ECONOMY

ART +
DESIGN +
ARCHITECTURE

SCIENCE +
TECHNOLOGY

CROSSOVER

DOCTORAL
DISSERTATIONS